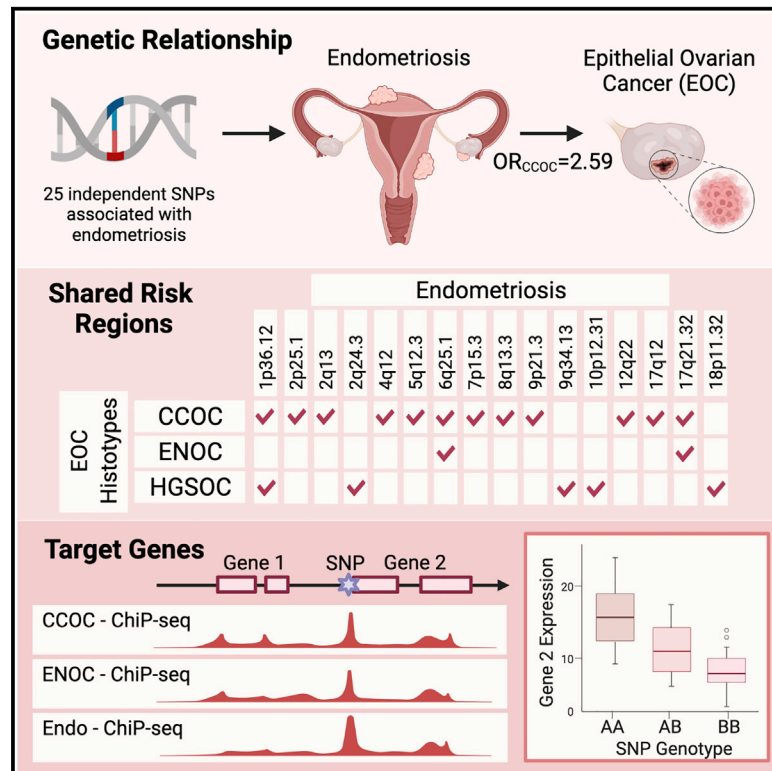


A multi-level investigation of the genetic relationship between endometriosis and ovarian cancer histotypes

Graphical abstract



Authors

Sally Mortlock, Rosario I. Corona, Pik Fang Kho, ..., Grant W. Montgomery, Kate Lawrenson, Siddhartha P. Kar

Correspondence

s.mortlock@imb.uq.edu.au

In brief

Mortlock et al. report a strong genetic relationship between endometriosis and epithelial ovarian cancers (EOCs) using genetic correlation, Mendelian randomization, bivariate GWAS, colocalization, and functional genomic analyses. Results increase our understanding of cross-disorder pathogenesis and yield pleiotropic targets to facilitate potential preventive pharmacological intervention and targeted EOC screening.

Highlights

- Endometriosis is genetically correlated with CCOC, ENOC, and HGSOC
- Genetic liability to endometriosis confers risk of these EOC histotypes
- Profound colocalization of genetic associations at endometriosis and EOC risk loci
- Functional annotation highlights shared target genes elucidating the genetic link



Article

A multi-level investigation of the genetic relationship between endometriosis and ovarian cancer histotypes

Sally Mortlock,^{1,19,*} Rosario I. Corona,² Pik Fang Kho,^{3,4} Paul Pharoah,^{5,6} Ji-Heui Seo,⁷ Matthew L. Freedman,^{7,8} Simon A. Gayther,⁹ Matthew T. Siedhoff,¹⁰ Peter A.W. Rogers,¹¹ Ronald Leuchter,¹² Christine S. Walsh,¹³ Ilana Cass,¹² Beth Y. Karlan,¹⁴ B.J. Rimel,¹² Ovarian Cancer Association Consortium, International Endometriosis Genetics Consortium, Grant W. Montgomery,¹ Kate Lawrenson,^{2,9,12,17,18} and Siddhartha P. Kar^{15,16,17,18}

¹The Institute for Molecular Bioscience, The University of Queensland, Brisbane, QLD 4072, Australia

²Women's Cancer Research Program at Samuel Oschin Comprehensive Cancer Institute, Cedars-Sinai Medical Center, Los Angeles, CA, USA

³Department of Genetics and Computational Biology, QIMR Berghofer Medical Research Institute, Brisbane, Queensland, Australia

⁴School of Biomedical Science, Faculty of Health, Queensland University of Technology, Brisbane, Queensland, Australia

⁵Centre for Cancer Genetic Epidemiology, Department of Public Health and Primary Care, University of Cambridge, CB1 8RN Cambridge, UK

⁶Centre for Cancer Genetic Epidemiology, Department of Oncology, University of Cambridge, CB1 8RN Cambridge, UK

⁷Department of Medical Oncology, Dana-Farber Cancer Institute, Boston, MA, USA

⁸Center for Functional Cancer Epigenetics, Dana-Farber Cancer Institute, Boston, MA, USA

⁹Center for Bioinformatics and Functional Genomics, Samuel Oschin Comprehensive Cancer Institute, Cedars-Sinai Medical Center, Los Angeles, CA, USA

¹⁰Division of Minimally Invasive Gynecologic Surgery, Department of Obstetrics and Gynecology, Cedars-Sinai Medical Center, Los Angeles, CA, USA

¹¹University of Melbourne Department of Obstetrics and Gynaecology, and Gynaecology Research Centre, Royal Women's Hospital, Parkville, VIC 3052, Australia

¹²Division of Gynecologic Oncology, Department of Obstetrics and Gynecology, Cedars-Sinai Medical Center, Los Angeles, CA, USA

¹³Department of Obstetrics and Gynecology, University of Colorado, Aurora, CO, USA

¹⁴Department of Obstetrics and Gynecology, David Geffen School of Medicine, University of California, Los Angeles, CA, USA

¹⁵Medical Research Council Integrative Epidemiology Unit, University of Bristol, BS8 2BN Bristol, UK

¹⁶Population Health Sciences, Bristol Medical School, University of Bristol, BS8 2BN Bristol, UK

¹⁷These authors contributed equally

¹⁸Senior author

¹⁹Lead contact

*Correspondence: s.mortlock@imb.uq.edu.au

<https://doi.org/10.1016/j.xcrm.2022.100542>

SUMMARY

Endometriosis is associated with increased risk of epithelial ovarian cancers (EOCs). Using data from large endometriosis and EOC genome-wide association meta-analyses, we estimate the genetic correlation and evaluate the causal relationship between genetic liability to endometriosis and EOC histotypes, and identify shared susceptibility loci. We estimate a significant genetic correlation (r_g) between endometriosis and clear cell ($r_g = 0.71$), endometrioid ($r_g = 0.48$), and high-grade serous ($r_g = 0.19$) ovarian cancer, associations supported by Mendelian randomization analyses. Bivariate meta-analysis identified 28 loci associated with both endometriosis and EOC, including 19 with evidence for a shared underlying association signal. Differences in the shared risk suggest different underlying pathways may contribute to the relationship between endometriosis and the different histotypes. Functional annotation using transcriptomic and epigenomic profiles of relevant tissues/cells highlights several target genes. This comprehensive analysis reveals profound genetic overlap between endometriosis and EOC histotypes with valuable genomic targets for understanding the biological mechanisms linking the diseases.

INTRODUCTION

Endometriosis is a chronic gynecological disease affecting up to 12% of reproductive-age women.^{1–3} The disease is characterized by the presence of endometriotic lesions outside the uterus and is

associated with pelvic pain and subfertility.² Lesions are frequently categorized according to lesion location and depth of infiltration into the surrounding tissue and include superficial peritoneal lesions, deep infiltrating disease, and cysts (endometriomas), most commonly found on the ovary.⁴ While endometriosis



Table 1. Genetic correlation (r_g) between endometriosis and EOC histotypes estimated using linkage disequilibrium score regression and HDL

EOC histotype	LDSC		HDL	
	r_g (SE)	p	r_g (SE)	p value
Clear cell	0.71 (0.26)	0.007	0.58 (0.10)	1.01×10^{-8}
Endometrioid	0.48 (0.20)	0.016	0.42 (0.10)	4.20×10^{-5}
High-grade serous	0.19 (0.09)	0.033	0.13 (0.06)	0.018
Low-grade serous	NA	NA	0.10 (0.07)	0.158
Low malignant potential serous	0.88 (0.85)	0.401	0.23 (0.09)	7.21×10^{-3}
Mucinous	-0.18 (0.15)	0.227	0.08 (0.07)	0.31

LDSC, linkage disequilibrium score; SE, standard error.

is a benign condition, it shares features with cancer, including metastatic-like behavior, tissue invasion, proliferation, angiogenesis, and decreased apoptosis. Large epidemiologic studies have reproducibly shown that women with endometriosis have increased risk of epithelial ovarian cancer (EOC; standardized incidence ratio = 1.8–8.95), although the absolute risks are quite small, and there is currently no way to predict which endometriosis patients are most likely to develop EOC later in life.^{5–7} Somatic mutations shared between benign endometriotic lesions and adjacent tumors suggest these lesions are cellular precursors to endometriosis-associated EOCs. Examples include loss of function mutations in *ARID1A* and gain of function mutations in *PIK3C*.^{8–10}

Ovarian cancer is the deadliest gynecologic cancer. Fewer than 50% of women survive beyond 5 years after diagnosis due to the rapid development of chemoresistance and the absence of effective early detection strategies. Research is needed to advance understanding of disease etiology, identify risk factors, and develop early detection methods and effective targeted therapies. The major histological subtypes of EOC include high-grade serous (HGSOC), low-grade serous (LGSOC), mucinous (MOC), endometrioid (ENOC), and clear cell (CCOC) EOC. Borderline tumors of low malignant potential also exist, most typically with serous (LMPSOC) or mucinous differentiation. CCOC and ENOC are the two histotypes most strongly and reproducibly associated with endometriosis.^{11–13} Concurrent endometriosis is observed in 21%–51% of patients with CCOC and 23%–43% women with ENOC.^{14–16} These histotype-associations are supported by observational study data from 7,911 women with invasive EOC in the Ovarian Cancer Association Consortium that showed a significant association between history of endometriosis and specific histological subtypes of EOC, including CCOC (odds ratio [OR] = 3.05), ENOC (OR = 2.04) and, to a lesser extent, LGSOC (OR = 2.11).¹³

Recent genome-wide association studies (GWASs) have provided strong evidence for a genetic contribution to risk of both endometriosis and EOC. A total of 19 independent genomic regions have been associated with endometriosis risk and 34 have been associated with different histotypes of EOC.^{17,18} Germline variants may also contribute to increased risk of developing both diseases. Lu et al.¹⁹ used genetic data from 84,000 single-nucleotide polymorphisms (SNPs) genotyped in EOC (10,065 cases) and endometriosis (3,194 cases) cohorts to estimate the genetic correlation between the diseases and found a

strong significant genetic correlation between endometriosis and CCOC (0.51), ENOC (0.48), and LGSOC (0.40) and smaller correlation with high-grade serous ovarian cancer (HGSOC) (0.25). That study, however, was limited by the relatively small number of SNPs and sample numbers and did not provide evidence for a causal relationship between genetic liability to endometriosis and EOC risk or shared risk loci. The aim of the present study was to use data from more recent and larger endometriosis (14,949 cases/190,715 controls) and EOC (25,509 cases/40,941 controls) GWAS meta-analyses and a battery of state-of-the-art genetic methods to evaluate the relationship between endometriosis and EOC histotypes. We used Mendelian randomization (MR) to demonstrate that genetic liability to endometriosis was causally associated with histotype-specific EOC risk and established directionality from endometriosis to EOC risk rather than vice versa. We then evaluated the genetic relationship between endometriosis and EOC histotypes to identify shared risk loci, candidate functional target genes, and pathways.

RESULTS

Genetic correlation between endometriosis and ovarian cancer histotypes

Genetic correlation can be used to describe the genetic relationship between two traits and is an estimate of the proportion of variance that two traits share that is attributed to genetics. Estimating the genetic correlation between traits contributes to our understanding of shared underlying genetic risk factors and biological pathways. To estimate the genetic correlation between EOC histotypes and endometriosis, we used GWAS summary statistics from meta-analyses conducted by Phelan et al.¹⁸ and Sapkota et al.¹⁷ respectively, and linkage disequilibrium (LD) score regression (LDSC).²⁰ SNPs were matched on position and alleles to ensure effect size estimates were harmonized across datasets to obtain a set of 7,617,581 SNPs represented in the EOC histotypes and endometriosis datasets. We estimated significant ($p < 0.05$) positive genetic correlations (r_g) between endometriosis and CCOC ($r_g = 0.71$), ENOC ($r_g = 0.48$), and HGSOC ($r_g = 0.19$) (Table 1). The r_g for genetic correlation with LMPSOC was 0.88 but this did not reach statistical significance, and we were unable to estimate r_g for LGSOC due to this histotype having the smallest sample size (1,012 cases). Genetic correlation between the diseases was also estimated using

Table 2. MR results considering genetic liability to endometriosis as the exposure and EOC histotypes as the outcome

EOC histotype	MR method	OR (95% CI)	p	MR-PRESSO global test p	MR-Egger intercept test p
High-grade serous	IVW	1.22 (1.07–1.38)	0.002	<0.001	0.95
	weighted median	1.16 (1.02–1.32)	0.025		
	MR-Egger	1.23 (0.82–1.86)	0.319		
	MR-PRESSO ^a	1.22 (1.09–1.35)	0.004		
Low-grade serous	IVW	1.27 (0.96–1.67)	0.091	0.281	0.368
	weighted median	1.27 (0.87–1.84)	0.212		
	MR-Egger	0.86 (0.35–2.09)	0.742		
Low malignant potential serous	IVW	1.45 (1.17–1.79)	0.001	0.167	0.943
	weighted median	1.52 (1.16–1.99)	0.003		
	MR-Egger	1.42 (0.71–2.83)	0.323		
Mucinous	IVW	1.24 (1–1.53)	0.046	0.508	0.217
	weighted median	1.03 (0.77–1.39)	0.821		
	MR-Egger	0.83 (0.42–1.63)	0.583		
Endometrioid	IVW	1.66 (1.42–1.93)	1.4E-10	0.867	0.954
	weighted median	1.58 (1.27–1.97)	3.0 × 10 ⁻⁵		
	MR-Egger	1.63 (1–2.67)	0.051		
Clear cell	IVW	2.59 (2.09–3.21)	2.8 × 10 ⁻¹⁸	0.786	0.951
	weighted median	2.48 (1.82–3.39)	9.6 × 10 ⁻⁸		
	MR-Egger	2.54 (1.28–5.02)	0.007		

CI, confidence interval; OR, odds ratio.

Results for the MR-PRESSO global and MR-Egger intercept tests for the detection of pleiotropy.

^aMR-PRESSO result after removal of the outlier variant rs1802669.

high-definition likelihood inference (HDL),²¹ which has been shown to reduce the variance of the estimate by fully accounting for LD. Genetic correlation estimates generated using HDL were consistent with LDSC, identifying a significant correlation between endometriosis and CCOC ($r_g = 0.58$), ENOC ($r_g = 0.42$), HGSOC ($r_g = 0.13$), and LMPSOC ($r_g = 0.23$) (Table 1). There was no evidence of a significant correlation between either MOC or LGSOC and endometriosis.

MR analysis

We then used MR based on the inverse-variance weighted (IVW) method²² and sensitivity analyses based on the weighted median²³ and Mendelian randomization-Egger (MR-Egger)²⁴ methods, which involve models that are more robust to horizontal pleiotropy, to investigate the association between genetic liability to endometriosis and EOC histotypes. Genetic liability to endometriosis as predicted by 25 independent genome-wide significant²⁵ ($p < 5 \times 10^{-8}$) endometriosis lead SNPs was associated with increased risk of CCOC, ENOC, HGSOC, and LMPSOC in the IVW analysis and the results were consistent in sensitivity analyses (Table 2). The strongest associations were observed for ENOC ($p = 1.4 \times 10^{-10}$, OR = 1.66 [1.42–1.93]) and CCOC ($p = 2.8 \times 10^{-18}$, OR = 2.59 [2.09–3.21]). Next, we applied the Mendelian Randomization Pleiotropy Residual Sum and Outlier (MR-PRESSO) MR method, which includes a test for the detection of horizontal pleiotropy, outlier (potentially pleiotropic) SNP removal if pleiotropy is detected, and a test to detect distortion of the MR estimate after removal of outlier SNPs.²⁶ MR-PRESSO did not yield evidence of horizontal pleiotropy in any of our MR analyses except for the

endometriosis to HGSOC association, wherein outlier removal did not significantly alter the MR estimate (Table 2). The MR-Egger intercept test²⁴ also did not identify any statistical evidence of pleiotropy (Table 2). Finally, we did not find any evidence for bidirectional associations; i.e., genetic liability to EOC histotypes was not associated with endometriosis risk (Table S1).

Genetic associations shared between endometriosis and ovarian cancer histotypes

To identify genetic associations with some evidence of a shared contribution from both diseases, we combined the EOC histotypes and endometriosis susceptibility datasets using two complementary approaches; first, meta-analysis using approximate Bayes factors computed and combined by the Meta-Analysis with an Approximate Bayes Factor (MetABF) method in both an independent and fixed model,²⁷ and, second, meta-analysis based on the modified Han and Eskin random-effects model and fixed-effects model implemented in the modified random effects model (RE2C).^{28,29} The cross-trait meta-analysis identified several genome-wide significant associations, and a summary of the number of SNPs nominally associated with both endometriosis and each EOC histotype using MetABF and RE2C are listed in Table 3. SNPs were considered as markers of a shared genetic association with both traits if they had (1) a \log_{10} approximate Bayes factor (ABF) >4 in the cross-trait MetABF analysis using either model, (2) a p value < 5×10^{-8} in the cross-trait RE2C analysis using either model, and (3) a p value < 0.05 in each single trait meta-analysis. A combined \log_{10} ABF >4 is equivalent to a posterior probability of combined association >90% given a prior

Table 3. Number of significant SNPs and genomic loci identified in the EOC histotype and endometriosis cross-trait meta-analyses

EOC histotype that was combined with endometriosis	No. SNPs with ABF >4 in combined data	No. SNPs with RE2C $p < 5 \times 10^{-8}$ in combined data	No. of genomic loci significant in both MetABF and RE2C ^a
Clear cell	1,055	336	14
Endometrioid	759	309	6
High-grade serous	2,814	1,851	13
Low-grade serous	733	237	3
LMP serous	1,114	514	5
Mucinous	899	365	5

LMP, low malignant potential.

^aThe number of genomic loci significant in both MetABF and RE2C reported here is the set of loci where the lead SNPs achieved ABF > 4 and RE2C $p < 5 \times 10^{-8}$ in the combined data and had nominal evidence of association ($p < 0.05$) in each individual GWAS dataset (i.e., in the endometriosis dataset and in the corresponding EOC histotype dataset). Independent loci were identified by linkage disequilibrium-based pruning at $r^2 < 0.6$.

probability of association at any SNP of one in 1,000. All SNPs ($n = 2,237$ non-redundant) with p value $< 5 \times 10^{-8}$ in RE2C had \log_{10} ABF > 4 in MetABF, suggesting good consistency between the methods. Filtering out SNPs that did not have evidence for nominal association in each single-trait meta-analysis ($p < 0.05$) filtered out ~68% of the 3,612 SNPs, leaving 1,144 SNPs that met all three aforementioned criteria. The largest number of shared genome-wide significant loci (or regions) were identified between endometriosis and CCOC (14 loci; Tables 3 and 4). This was followed by 13 risk loci shared between endometriosis and HGSOE, six risk loci with ENOC, five risk loci with MOC, five risk loci with LMPSOC, and three risk loci with LGSOC (Tables 3 and 4). Four loci had lead SNPs with opposite directions of allelic association between endometriosis and the EOC histotype (Table 4). Significant SNPs in each analysis are listed in Table S2. Several loci also contain lead SNPs that have been associated with other reproductive traits and diseases including uterine fibroids, sex hormone levels, polycystic ovarian syndrome (PCOS), and age at menarche (Table S3).

Colocalization analyses to identify shared candidate causal variants

Our MetABF and RE2C analyses identified shared susceptibility loci for endometriosis and EOC. However, it is not clear whether the same candidate causal variants underlie the associations at these loci or whether the associations at these loci are driven by distinct candidate causal variants for endometriosis and EOC. We examined the underlying shared genetic architecture of endometriosis and EOC further using a statistical model to estimate the posterior probability of association (PPA) that a genomic region (1) contains a variant associated only with endometriosis (PPA₁), (2) contains a variant associated only with EOC (PPA₂), (3) contains a variant associated with both traits (PPA₃), and (4) contains both a variant associated with endometriosis and an independent variant associated with EOC (PPA₄). These models were implemented in GWAS-PW (pairwise analysis of GWAS).³⁰ Genomic regions with a PPA₃ > 0.5, evidence of the same candidate causal variants influencing both diseases, or PPA₄ > 0.5, evidence that the candidate causal variants underlying the association with each trait were distinct, are listed in Table 5. CCOC had the largest number of genomic regions ($n = 13$) with evidence of shared causal variants

with endometriosis. All regions identified with PPA₃ or PPA₄ > 0.5 contained lead SNPs significant in the cross-trait meta-analyses (\log_{10} ABF > 4 in the cross-trait MetABF analysis, $p < 5 \times 10^{-8}$ in the cross-trait RE2C analysis and $p < 0.05$ in each single-trait meta-analysis) except for one region on chromosome 3 (Chr 3:126,215,130–128,194,265) where only colocalization offered evidence for a shared association between MOC and endometriosis. Two regions with PPA₃ > 0.5 that achieved genome-wide significance in the meta-analyses ($p < 5 \times 10^{-8}$ and \log_{10} ABF > 4) were >1 Mb from any risk locus previously reported for endometriosis and EOC: 2q24.3 (rs13000026) and 18p11.31 (rs10048393). One of the four loci (9p21) with lead SNPs with opposite directions of effect, identified in the cross-trait meta-analysis between endometriosis and CCOC, also had evidence for the same causal variant underpinning both diseases from the colocalization analysis. Another on chromosome 17 (17q12) had evidence for two distinct signals for endometriosis and HGSOE. The remaining two had no evidence of colocalization. Several genomic regions containing genome-wide significant associations identified in the cross-trait meta-analyses only achieved PPA_{1/2} > 0.5, suggesting the associations were only driven by one of the two traits. However, this can also occur due to the limited power to detect colocalization with the smaller sample sizes that were available for cross-trait colocalization analyses involving the less common EOC histotypes.

Gene-based association analysis of endometriosis and ovarian cancer histotypes

We conducted a gene-based association analysis using fast set-based association analysis (fastBAT),³¹ a statistical association test that calculates the combined association for all SNPs mapped to each gene while taking into account correlation between SNPs due to LD. Nine genes were associated at genome-wide significance ($p < 2.45 \times 10^{-6}$) with endometriosis (*GREB1*, *MIR4429*, *KDR*, *WNT4*, *SYNE1*, *CDKN2B-AS1*, *CDC42*, *ID4*, *PTPRO*), 67 with HGSOE, one with LGSOC (*KIAA1024*), four for LMPSOC (*TERT*, *SLC6A18*, *MIR4457*, *CLPTM1L*), and 27 for MOC in single-trait gene-based analysis (Table S4). Genome-wide significant genes for endometriosis were nominally significant ($p < 0.05$) for CCOC (*GREB1*, *MIR4429*, *WNT4*), ENOC (*CDKN2B-AS1*), and HGSOE (*CDKN2B-AS1*, *MIR4429*, *WNT4*) (Table S4).

Table 4. Lead SNPs in genomic loci that demonstrated shared associations with an EOC histotype and endometriosis from the RE2C meta-analyses

rsID	Chr	Pos ^a	ABF	Be	p value	RE2Cp	Pval_Ovarian	Pval_Endo	Nearest gene or gene with functional evidence
Clear cell ovarian cancer + endometriosis									
rs61768001	1	22,465,820	10.92	0.13	9.54×10^{-14}	1	2.03×10^{-2}	1.59×10^{-12}	LINC00339
rs11674184	2	11,721,535	13.27	-0.11	3.86×10^{-16}	1	3.02×10^{-3}	3.19×10^{-14}	GREB1
rs10167914	2	113,563,361	8.07	0.11	9.57×10^{-11}	1	2.59×10^{-4}	4.94×10^{-8}	IL1A
rs4516787	4	56,010,165	10.97	-0.11	9.10×10^{-14}	1	8.20×10^{-4}	1.88×10^{-11}	KDR
rs1311245	5	64,272,107	5.5	0.07	4.55×10^{-8}	1	2.27×10^{-2}	5.58×10^{-7}	CWC27
rs1971256	6	151,816,011	6.17	0.09	9.57×10^{-9}	1	3.20×10^{-2}	9.68×10^{-8}	CCDC170
rs17803970	6	152,553,718	6.83	-0.15	1.62×10^{-9}	1	2.40×10^{-3}	9.82×10^{-8}	SYNE1
rs71575922	6	152,554,014	8.04	0.12	1.01×10^{-10}	1	4.34×10^{-4}	2.02×10^{-8}	SYNE1
rs12700667	7	25,901,639	7.27	0.09	6.58×10^{-10}	1	1.18×10^{-2}	1.51×10^{-8}	AK057379
rs78103255	8	75,311,331	6.08	-0.09	1.19×10^{-8}	1	6.64×10^{-4}	2.47×10^{-6}	GDAP1
rs566679 ^{b,c}	9	22,634,893	6.26	0.07	2.60×10^{-5}	2.10×10^{-8}	8.64×10^{-3}	6.62×10^{-8}	LINC01239
rs7309252	12	95,687,497	5.69	0.07	2.84×10^{-8}	1	4.53×10^{-3}	1.07×10^{-6}	VEZT
rs11651755 ^b	17	36,099,840	6.08	0.05	4.52×10^{-5}	1	6.78×10^{-9}	2.02×10^{-2}	HNF1B
rs8069263	17	46,286,778	5.54	0.07	4.10×10^{-8}	8.03×10^{-8}	3.86×10^{-2}	3.88×10^{-7}	SKAP1
Endometrioid ovarian cancer + endometriosis									
rs56318008	1	22,470,407	10.11	0.12	6.77×10^{-13}	1	3.37×10^{-2}	3.50×10^{-12}	LINC00339
rs495590	1	172,122,809	5.7	0.08	2.97×10^{-8}	1	2.00×10^{-4}	2.42×10^{-5}	DNM3
rs1971256	6	151,816,011	7.36	0.1	5.28×10^{-10}	1	1.26×10^{-3}	9.68×10^{-8}	CCDC170
rs6475610	9	22,141,894	8.39	0.08	4.33×10^{-11}	1	7.29×10^{-3}	1.73×10^{-9}	CDKN2B-AS1
rs11031005	11	30,226,356	7.39	-0.11	4.94×10^{-10}	1	1.06×10^{-3}	1.03×10^{-7}	FSHB
rs10445377	17	46,214,168	6.66	0.08	2.71×10^{-9}	1	1.95×10^{-3}	3.20×10^{-7}	SKAP1
High-grade serous ovarian cancer + endometriosis									
rs12037376 ^b	1	22,462,111	10.99	0.1	3.15×10^{-13}	3.06×10^{-14}	3.51×10^{-3}	1.04×10^{-12}	LINC00339
rs7570979	2	11,717,429	7.76	0.08	1.91×10^{-10}	1	6.59×10^{-3}	1.43×10^{-9}	GREB1
rs13000026	2	165,558,884	7.03	-0.07	1.08×10^{-9}	1	1.10×10^{-5}	2.27×10^{-5}	COBLL1
rs1250244 ^b	2	216,297,796	5.57	-0.07	1.36×10^{-7}	1.61×10^{-8}	2.69×10^{-2}	8.73×10^{-8}	FN1
rs6908034 ^{b,c}	6	19,773,930	7.23	0.04	2.25×10^{-3}	1.65×10^{-9}	2.21×10^{-2}	2.09×10^{-9}	ID4
rs111610638	6	152,449,994	5.54	-0.15	3.65×10^{-8}	1	1.84×10^{-3}	3.90×10^{-6}	SYNE1
rs1981046	9	22,173,407	5.44	-0.06	4.66×10^{-8}	1	2.31×10^{-2}	1.03×10^{-7}	CDKN2B-AS1
rs635634 ^b	9	136,155,000	10.64	0.09	9.40×10^{-13}	6.92×10^{-14}	2.25×10^{-11}	3.39×10^{-4}	ABO
rs7084454	10	21,821,274	10.39	0.08	3.50×10^{-13}	1	2.77×10^{-9}	9.06×10^{-6}	MLLT10
rs11658063 ^{b,c}	17	36,103,872	7.87	-0.03	1.50×10^{-2}	2.98E-10	3.63×10^{-10}	1.83×10^{-2}	HNF1B
rs62065444 ^b	17	43,565,599	11.11	0.12	2.08×10^{-13}	2.68×10^{-14}	1.20×10^{-13}	4.77×10^{-2}	PLEKHM1
rs7217120 ^b	17	46,484,755	13.5	0.09	7.96×10^{-15}	1.08×10^{-16}	2.08×10^{-14}	3.69×10^{-4}	SKAP1
rs10048393	18	3,476,253	5.62	0.06	3.09×10^{-8}	1	2.12×10^{-5}	3.23×10^{-4}	AX721193
Low-grade serous ovarian cancer + endometriosis									
rs77294520	2	11,660,955	10.72	0.15	1.39×10^{-13}	1	4.70×10^{-2}	9.91×10^{-13}	GREB1
rs584336 ^{b,c}	6	152,616,173	6.35	0.07	4.28×10^{-6}	1.61×10^{-8}	1.11×10^{-2}	4.17×10^{-8}	SYNE1
rs10445377	17	46,214,168	5.72	0.08	2.69×10^{-8}	1	1.90×10^{-2}	3.20×10^{-7}	SKAP1
LMP serous ovarian cancer + endometriosis									
rs4654785	1	22,491,843	6.78	0.09	2.18×10^{-9}	1	3.78×10^{-2}	1.89×10^{-8}	LOC105376850
rs10748858 ^b	10	105,639,514	5.81	0.07	6.06×10^{-7}	1.30×10^{-8}	1.09×10^{-6}	5.31×10^{-4}	OBFC1
rs11031005	11	30,226,356	6.24	-0.11	8.14×10^{-9}	1	2.73×10^{-2}	1.03×10^{-7}	FSHB
rs10445377	17	46,214,168	7.46	0.08	4.06×10^{-10}	1	4.56×10^{-5}	3.20×10^{-7}	SKAP1
rs35713035 ^b	17	46,501,710	6.43	0.09	1.75×10^{-8}	1.74×10^{-9}	4.32×10^{-6}	3.60×10^{-5}	SKAP1

(Continued on next page)

Table 4. Continued

rsID	Chr	Pos ^a	ABF	Be	p value	RE2Cp	Pval_Ovarian	Pval_Endo	Nearest gene or gene with functional evidence
Mucinous ovarian cancer + endometriosis									
rs11674184	2	11,721,535	12.11	-0.1	6.13×10^{-15}	1	3.23×10^{-2}	3.19×10^{-14}	<i>GREB1</i>
rs6546324	2	67,856,490	5.91	-0.08	1.71×10^{-8}	1	1.76×10^{-2}	3.02×10^{-7}	<i>LINC01812</i>
rs10167914	2	113,563,361	6.98	0.1	1.36×10^{-9}	1	7.23×10^{-3}	4.94×10^{-8}	<i>IL1A</i>
rs4849174 ^b	2	113,973,467	12.14	0.09	2.66×10^{-9}	2.00×10^{-15}	2.53×10^{-14}	2.89×10^{-3}	<i>PAX8</i>
rs67808862 ^b	3	138,849,543	10.26	0.07	5.94×10^{-7}	2.53×10^{-13}	2.14×10^{-13}	4.64×10^{-2}	<i>BPESC1</i>

ABF, logarithm (base 10) approximate Bayes factor Be, Estimated beta coefficient from the fixed-effects model; p value, fixed-effects model p value; RE2CP, RE2C p value (RE2Cp is 1 for SNPs where there is little or no evidence of heterogeneity across the two traits, and for such SNPs the fixed-effects model and its corresponding association p value become the model of choice).

^aSNP with significant heterogeneity and results presented from independent MetABF and RE2C random-effects model.

^bBuild 37 positions.

^cDirection of effect is different for each trait.

We looked at the overlap between the top 1% of genes associated with each trait (204/20,439 genes evaluated in the fastBAT analysis) and observed an overlap of 5% between endometriosis and HGSOE (11 genes), 4% with CCOC (nine genes), 3% with LMPSOC (seven genes), 3% with ENOC (six genes), 3% with MOC (five genes), and 1% with LGSOC (two genes). Two genes, *SNX11* and *CBX1*, were associated with endometriosis, ENOC, HGSOE, and LMPSOC. *SKAP1* was associated with HGSOE, LMPSOC, and endometriosis. However, none of the genes in the top 1% that overlapped between endometriosis and CCOC were in the top 1% of genes associated with other histotypes. Using an over-representation analysis in WebGestalt,³² no specific pathways were significantly enriched (false discovery rate [FDR] <0.05) for overlapping genes. This was also the case when the analysis was extended to the top 5% of genes associated with each trait and the overlapping genes between endometriosis and each EOC histotype in the top 5% considered (Table S4).

Functional annotation

We collated all candidate causal variants by identifying all SNPs in tight LD with the lead SNPs ($r^2 > 0.7$) from the cross-trait meta-analyses (\log_{10} ABF >4 in the cross-trait MetABF analysis, $p < 5 \times 10^{-8}$ in the cross-trait RE2C analysis, and $p < 0.05$ in each single trait meta-analysis). The set of candidate causal variants included 4,044 unique SNPs, which we functionally annotated to genes and epigenomic biofeatures.

Overlap with noncoding DNA biofeatures

To identify putative functional SNPs, we overlapped all candidate causal SNPs with noncoding regulatory elements (biofeatures) identified by epigenomic profiling of disease-relevant tissues and cell lines. The biofeature catalog consisted of 11 consensus peak sets (see STAR Methods, Table S5) derived from 45 epigenomic profiles. Epigenome features included open chromatin (18 Assay of Transposase Accessible Chromatin sequencing [ATAC-seq] datasets) and active chromatin (27H3K27ac chromatin immunoprecipitation sequencing [ChIP-seq] profiles; Table S5). The specimens profiled included non-cancerous gynecologic tissues (fallopian tube, endometriosis, and endometriosis-associated stroma) and EOC (clear cell, endometrioid, high-grade serous, and mucinous) tissues or cell line models.^{33,34} Consensus

peak sets averaged 33.6 (standard deviation (SD) = 22, range = [9, 84.3]) thousand peaks spanning, on average, 1.04% of the human genome (SD = 0.37, range = [0.42, 1.53]) (Figures S1A–S1C, Table S5). Genome coverage was marginally correlated with number of donors (Spearman's rho = 0.43, $p = 0.18$; Figures S1D–S1F).

We reduced the 1,144 candidate SNPs to 824 non-redundant variants most strongly associated with both endometriosis and EOC histotypes (\log_{10} ABF >4 in the cross-trait MetABF analysis, a p value < 5×10^{-8} in the cross-trait RE2C analysis, and a p value <0.05 in each individual trait meta-analysis). Of these 824 candidate causal variants, 119 (14.4%) overlapped at least one biofeature (Figure 1A; Table S6). The proportion of independent loci containing SNPs intersecting with biofeatures varied by EOC histotype, with only 33.3% of loci associated with endometriosis plus LGSOC overlapping at least one biofeature, while 71.4% of endometriosis and CCOC loci overlapped one or more relevant biofeatures (Figure 1B, Figures S2A–S2F; Table S7). As expected, ATAC-seq consensus peak sets provided different information compared with H3K27ac ChIP-seq peak sets. We observed that H3K27ac ChIP-seq consensus peak sets for fallopian tube, endometriosis-associated stroma, and endometriosis primary tissues and ATAC-seq consensus peaks for CCOC and fallopian tube intersected a similar set of SNPs, possibly reflecting the epidemiologic links between these tissues and diseases (Figure S3).

The 119 SNPs that overlapped at least one consensus peak set were distributed across 28 distinct loci (Table S6). Overlaps provided functional evidence that these SNPs in risk loci shared between endometriosis and EOC histotypes were located within regulatory regions. The *MLLT10* and *FSHB* loci contained the SNPs with the most functional evidence and highest number of overlaps, rs4071559 and rs10828247, each overlapping 11 biofeatures (Table S6). The *VEZT* locus harbored the SNPs with the second highest number of overlaps, where rs6538618 overlapped 10 biofeatures at the putative bidirectional *VEZT/FGD6* promoter (Figure 1C). SNP rs6538618 had additional functional evidence and has been associated with the expression of both *VEZT* and *FGD6* in endometrium,³⁵ fibroblasts, artery, and muscle tissue³⁶ (Figure 1C). *SKAP1* and *PAX8* contained the greatest number of SNPs overlapping biofeatures (26 SNPs).

Table 5. GWAS-PW results for analyses between EOC histotypes and endometriosis. Posterior probabilities of GWAS-PW models

EOC histotype	Chr	Region (pos ^a)	PPA_1	PPA_2	PPA_3	PPA_4
Clear cell	1	21,736,898:23,086,667	0.3	0	0.69	0.01
Clear cell	2	10,298,766:12,418,752	0.07	0	0.93	0
Clear cell	2	110,857,126:113,921,639	0.01	0	0.99	0
Clear cell	4	55,429,886:56,547,412	0.03	0	0.97	0
Clear cell	5	63,968,304:65,910,972	0.26	0	0.72	0.01
Clear cell	6	150,256,048:151,912,653	0.31	0	0.63	0.01
Clear cell	6	151,912,703:153,093,958	0.06	0	0.93	0
Clear cell	7	25,077,628:25,909,208	0.32	0	0.67	0.01
Clear cell	8	73,817,199:75,444,858	0.04	0	0.95	0
Clear cell	9	22,206,559:24,157,796	0.17	0	0.81	0
Clear cell	12	94,514,787:96,019,818	0.13	0	0.85	0
Clear cell	17	34,812,273:36,808,793	0	0.01	0.97	0.01
Clear cell	17	45,876,022:47,516,523	0.37	0	0.61	0.01
Endometrioid	6	150,256,048:151,912,653	0.42	0	0.54	0
Endometrioid	17	45,876,022:47,516,523	0.46	0	0.53	0.01
High-grade serous	1	21,736,898:23,086,667	0.16	0	0.7	0.15
High-grade serous	2	10,298,766:12,418,752	0.37	0	0.06	0.57
High-grade serous	2	165,178,853:167,160,029	0.02	0	0.89	0.03
High-grade serous	6	151,912,703:153,093,958	0.35	0	0.05	0.6
High-grade serous	9	135,298,917:137,040,737	0	0	0.97	0.03
High-grade serous	10	19,717,815:22,772,115	0	0	0.99	0.01
High-grade serous	17	34,812,273:36,808,793	0	0.02	0.43	0.55
High-grade serous	17	43,056,905:45,875,506	0	0.04	0.18	0.78
High-grade serous	17	45,876,022:47,516,523	0	0	0.06	0.94
High-grade serous	18	1,943,138:3,890,554	0.02	0	0.76	0.06
LMP serous	10	104,380,686:106,694,980	0.01	0.01	0.92	0.04
LMP serous	17	45,876,022:47,516,523	0.02	0	0.73	0.25
Mucinous	2	113,922,276:116,772,246	0	0.11	0.87	0.03
Mucinous	3	126,215,130:128,194,265	0.4	0	0.53	0.02

PPA_1, posterior probability of model 1 (association only to endometriosis); PPA_2, posterior probability of model 2 (association only to EOC); PPA_3, posterior probability of model 3 (shared association to both phenotypes) PPA_4, posterior probability of model 4 (two distinct associations, one to each phenotype).

^aBuild 37 positions.

Tissue-specific effects and disease-relevant pathways

Using functional mapping and annotation (FUMA),³⁷ we identified that the expression of genes containing, or nearby to, SNPs shared between endometriosis and two EOC histotypes (CCOC and HGSOE) clustered across reproductive tissues including ovary, fallopian tube, and uterus (Figures S4A–S4C). Several pathways were enriched within the set of genes annotated to significant SNPs (Table S8). Unlike the fastBAT analysis, genes were not identified using a gene-based association analysis (SNPs within gene) but were instead annotated based on position (gene within 10 kb of an SNP). Focusing on enriched pathways containing three or more genes, pathways related to cell adhesion and nuclear division were enriched for genes annotated to SNPs associated with both endometriosis and CCOC. Gene sets associated with other reproductive traits and diseases were also enriched, including uterine fibroids, endometrial cancer, dysmenorrheic pain severity, and gestational age at birth (Table S8).

Causal associations with gene expression and methylation

The fastBAT analysis involved a purely statistical gene-level association test. To complement fastBAT, we used summary-data-based Mendelian randomization (SMR),³⁸ which integrates gene-level expression and methylation with the GWAS data to elucidate potential gene-level functional mechanisms. SMR enabled the identification of potentially causal associations between shared susceptibility to endometriosis and EOC histotypes and gene expression using SNPs associated with the traits from their individual GWAS meta-analyses. We performed an SMR analysis using summary statistics from the endometriosis and each of the EOC histotype GWAS meta-analyses, and expression quantitative trait locus (eQTL) data (eQTL p value < 5 × 10⁻⁸) from endometrium,^{35,39} blood,⁴⁰ and Genotype-Tissue Expression (GTEx) uterus and ovary³⁶ (Table S9). When restricted to regions with evidence of a shared variant associated with both

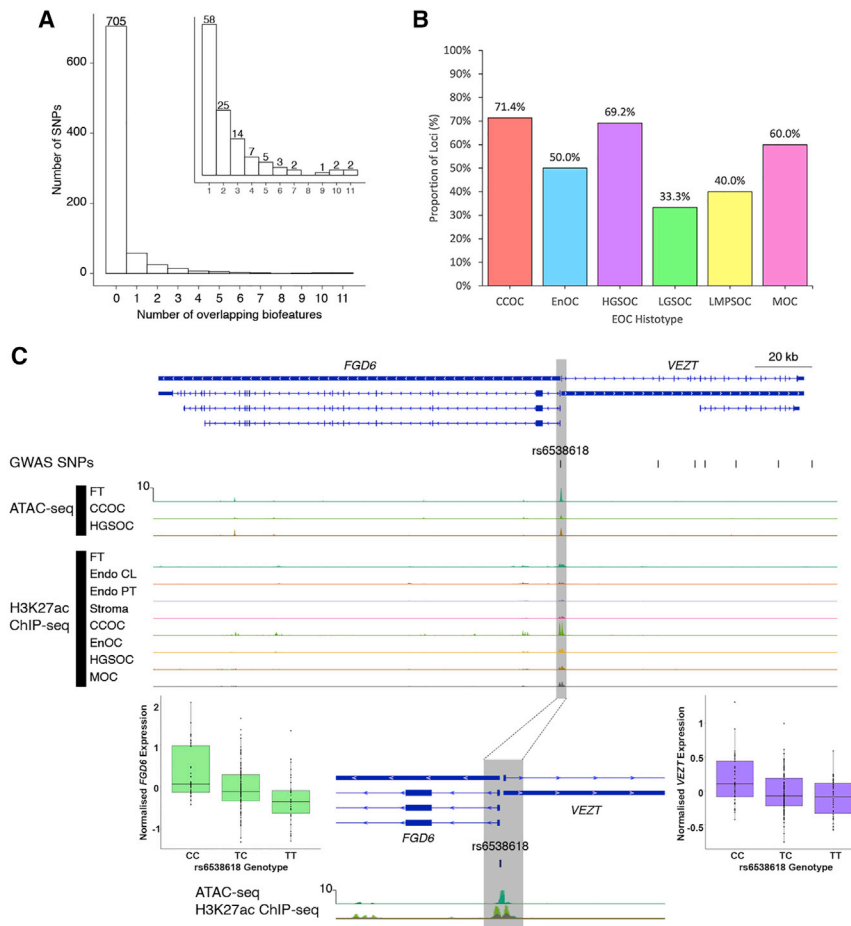


Figure 1. Functional annotation of SNPs associated with risk of endometriosis and epithelial ovarian cancer

(A) Histogram of number of non-redundant SNPs for all epithelial ovarian cancer (EOC) histological subtypes that overlap n biofeatures. Inset: histogram of number of non-redundant SNPs for all histological subtypes that overlap at least one biofeature.

(B) Proportion of loci shared between endometriosis and each EOC histotype containing SNPs that overlap at least one biofeature.

(C) A promoter SNP at the *VEZT/FGD6* locus overlaps 10 biofeatures and intersects with an active open region of chromatin that lies in a bidirectional promoter associated with these two genes. Biofeatures are shown as peaks on the ATAC-seq and H3K27ac ChIP-seq tracks for primary tissues and cell lines. Endo, endometriosis; FT, fallopian tube; Stroma, endometriosis-associated stroma; CCOC, clear cell ovarian cancer; CL, cell lines; ENOC, endometrioid ovarian cancer; HGSOC, high-grade serous ovarian cancer; MOC, mucinous ovarian cancer; PT, primary tissues. Specimens are primary tissues unless otherwise indicated. The gray shaded area highlights peaks overlapping rs6538618. Boxplots show the association between rs6538618 genotypes and expression of *VEZT* and *FGD6* in endometrium.

endometriosis and an EOC histotype from the colocalization analysis (GWAS-PW $PPA_3 > 0.5$), SMR identified two gene-level associations (SMR p value < 0.05) based on expression in the endometrium: variants were associated with risk of endometriosis, HGSOC and expression of *LINC00339* (also known as *HSPC157*) and endometriosis, MOC and expression of *PAX8* (Table S9). The heterogeneity in dependent instruments (HEIDI)³⁸ test p value was > 0.05 for both these associations, indicating colocalization between expression-associated SNPs and risk SNPs associated with both diseases. No significant SMR associations were identified in uterus or ovary gene expression data from GTEx.

Previous studies have shown a large proportion of eQTLs are shared between tissues.^{35,36} To increase power, the analysis was repeated using a large blood *cis*-eQTL dataset from eQTL-Gen⁴⁰ ($n = 31,684$ individuals) and expression of seven genes was found to be associated (SMR p value < 0.05 ; HEIDI p value > 0.05) with both risk of endometriosis and EOC histotypes in the regions where there was evidence of a shared signal between the two diseases ($PPA_3 > 0.5$, Table S9). The expression of *NBPF3*, *GDAP*, and *SKAP1* was associated with risk of endometriosis and CCOC, while the expression of *AC018521.5*, *AC018521.5*, and *SP2-AS1* was associated with risk of endometriosis and ENOC in blood.

Significant associations (SMR p value < 0.05 ; HEIDI p value > 0.05) between variants, methylation in the endometrium, and risk of endometriosis and at least one EOC histotype were identified at six CpG sites, including those near the *GREB1* and *KDR* signals for endometriosis and CCOC (Table S9). Using a large blood methylation quantitative trait locus (mQTL) dataset⁴¹ for SMR analysis, we identified variants affecting methylation at 78 CpG sites where variants associated with methylation were also associated with endometriosis and at least one EOC histotype, including sites near *WNT4/LINC00339* for CCOC and HGSOC; *GREB1*, *FGD6*, *ESR1* for CCOC; *SKAP1* for ENOC and LMPSOC; and *MLL10* for HGSOC. Each of these methylation analyses was restricted to regions with evidence of a shared underlying association between endometriosis and an EOC histotype based on GWAS-PW ($PPA_3 > 0.5$) and the SMR HEIDI test ($p > 0.05$) filter further ensured colocalization between SNP-disease and SNP-methylation associations. Table 6 summarizes the various levels of evidence gained from the aforementioned analyses for loci associated with both endometriosis and EOC histotypes.

Finally, we evaluated the expression of putative target genes annotated in the cross-trait meta-analysis and identified by fast-BAT and SMR analyses in eight endometrial cell types profiled by single-cell RNA-sequencing⁴² (Figures S5A and S5B). Of these, *SYNE1*, *NFE2L1*, *GREB1*, *IDA*, and *KDR* were reported to be differentially expressed between eutopic and ectopic lesions from women with endometriosis and normal endometrium.^{43,44}

Table 6. Summary of evidence from the bivariate meta-analyses, GWAS-PW, overlap of biofeatures, fastBAT, and SMR for loci associated with both endometriosis and EOC histotypes

Risk SNP (cytoband)	Significant in meta-analysis	Colocalized signal	Feature overlap	fastBAT	SMR
rs495590 (1q24.3)	ENOC			<i>DNM3</i>	
rs61768001/rs12037376 (1p36.12)	CCOC, HGSOC	CCOC, HGSOC	5	<i>WNT4</i>	CpG site near <i>WNT4</i>
rs10167914 (2q13)	CCOC, MOC	CCOC	3	<i>IL1A</i>	
rs4849174 (2q13)	MOC	MOC	7	<i>PSD4</i>	
rs13000026 (2q24.3)	HGSOC	HGSOC			
rs11674184 (2p25.1)	CCOC, MOC	CCOC	2	<i>GREB1/MIR4429</i>	
rs7570979 (2p25.1)	HGSOC	HGSOC	2	<i>MIR4429</i>	
rs1250244 (2q35)	HGSOC		2		
rs4516787 (4q12)	CCOC	CCOC	1		
rs1311245 (5q12.3)	CCOC	CCOC	1		
rs6908034 (6p22.3)	HGSOC				
rs1971256 (6q25.1)	CCOC, ENOC	CCOC, ENOC	5	<i>CCDC170</i>	
rs17803970 (6q25.2)	CCOC	CCOC			
rs71575922 (6q25.2)	CCOC	CCOC			
rs111610638 (6q25.2)	HGSOC	HGSOC	1		
rs12700667 (7p15.2)	CCOC	CCOC	2		
rs78103255 (8q21.11)	CCOC	CCOC		<i>GDAP1</i>	<i>GDAP1</i> expression CpG Site near <i>GDAP1</i>
rs566679 (9p21.3)	CCOC	CCOC			
rs6475610 (9p21.3)	ENOC			<i>CDKN2B-AS1/CDKN2A</i>	
rs1981046 (9p21.3)	HGSOC			<i>CDKN2B-AS1</i>	
rs635634 (9q34.2)	HGSOC	HGSOC	4		CpG site near <i>ABO</i>
rs7084454 (10p12.31)	HGSOC	HGSOC	11	<i>MLLT10/CASC10/SKIDA1/DNAJC1</i>	CpG site near <i>MLLT10</i>
rs10748858 (10q24.33)	LMPsOC	LMPsOC		<i>OBFC1</i>	
rs11031005 (11p14.1)	ENOC, LMPsOC		11		
rs7309252 (12q22)	CCOC	CCOC	10	<i>VEZT</i>	
rs11651755 (17q12)	CCOC	CCOC	3		CpG site near <i>HNF1B</i>
rs11658063 (17q12)	HGSOC	HGSOC	3		
rs62065444 (17q21.31)	HGSOC	HGSOC			
rs8069263/rs10445377 (17q21.32)	CCOC, ENOC, LGSOC, LMPsOC	CCOC, ENOC, LMPsOC	2	<i>SKAP1/SNX11/CBX1/NFE2L1/LOC101927166</i>	CpG site near <i>HOXB8</i> CpG site near <i>SKAP1</i>
rs7217120 (17q21.32)	HGSOC	HGSOC	10	<i>SKAP1/SNX11/CBX1/NFE2L1/LOC101927166/HOXB2</i>	
rs35713035 (17q21.32)	LMPsOC	LMPsOC	3	<i>SKAP1/SNX11/CBX1/NFE2L1/LOC101927166</i>	<i>SKAP1</i> expression
rs10048393 (18p11.31)	HGSOC	HGSOC	1	<i>LOC100505592</i>	

Specifically, *ID4*, *FN1*, and *GREB1* were more highly expressed in stromal fibroblasts from ectopic lesions compared with eutopic endometrium, while *WNT4* and *CBX1* had lower expression in ectopic lesions.⁴³

DISCUSSION

Analysis of germline genetic risk association data from endometriosis and EOC GWAS meta-analyses provides evidence of a genetic correlation and causal relationship between endometri-

osis and CCOC, ENOC, and, to a lesser extent, HGSOC. Our results support epidemiological observations of an association between endometriosis and EOC as shown by estimates that women with endometriosis have two to three times higher risk of developing EOC^{13,45} and that a high proportion of CCOC and ENOC cases also have endometriosis (20%–50%).^{14–16} Historically, epidemiological studies have not found statistically significant evidence for an association between endometriosis and HGSOC. However, a 2015 analysis that involved evaluating genetic loci known at the time to be associated with endometriosis

risk in a smaller subset of the Ovarian Cancer Association Consortium case-control set used here found significant evidence, using a gene-based statistical test, of an association with both endometriosis and HGSOE risk at the 1p36 (*WNT4*) locus.⁴⁶ Our MR results are consistent with findings from Yarmolinsky et al.⁴⁷ However, potentially due to our use of a larger number of SNPs to instrument endometriosis (25 SNPs based on the latest endometriosis GWAS versus 10 SNPs in the previously published analysis), we find that point estimates of the effect size for all associations in our analysis are larger than those reported in Yarmolinsky et al. This is most notable in the OR for CCOC (2.6 versus 1.5). The associations presented here reinforce the well-established links between endometriosis and ENOCs and CCOCs, and we also observe an association between endometriosis and HGSOE that was maintained across more than one analytic approach, suggesting some shared pathways underlie the development of these two phenotypes.

Using cross-trait meta-analyses, we identified 28 distinct genomic loci that shared a lead variant contributing to the risk of both endometriosis and EOC histotypes. Colocalization analyses provided evidence ($PPA_3 > 0.5$) for a single causal association signal underlying risk for both endometriosis and EOC in 19 of these regions. Functional annotation revealed that 14 of these 19 loci also contained risk SNPs that overlapped active and/or open chromatin. The high posterior probability of colocalization at a large number of distinct loci is a remarkable feature of the genetic relationship between endometriosis and EOC histotypes and suggests that identifying target genes in these loci may be valuable to understand the link between endometriosis and EOC and to intervene in neoplastic transformation.

The associations and their directionality uncovered by our MR analyses when taken together with the shared genetics between endometriosis and EOC uncovered by the multiple other approaches suggests that vertical pleiotropy is likely the defining pleiotropic mechanism for these conditions. That is, genetic liability to endometriosis confers risk of specific EOC histotypes, endometriosis and EOC are biologically related, and a genetic variant's effect on endometriosis is likely to cause its effect on EOC for the variants highlighted in this study. This stands in contrast to horizontal pleiotropy, wherein the same genetic variants affect two traits independently, and may regulate common molecular processes implicated in both traits, but there is little direct biological relationship between the traits, which would have been the case had we not identified any association between endometriosis and EOC in MR analyses.

Combining GWAS data for conditions known to predispose to cancers and for the corresponding cancers themselves has previously helped identify novel susceptibility loci for nevus density and melanoma⁴⁸ and for gastroesophageal reflux disease and esophageal cancer.⁴⁹ Our analysis identified two risk loci not previously reported both in the context of endometriosis and EOC histotypes (i.e., >1 Mb away from any previously identified locus). At the first locus, located at chromosome2q24.3, the index SNP (rs13000026) lies intronic to *Cordon-bleu protein-like 1 (COBLL1)*, and at the second locus at 18p11.31, index SNP rs10048393 lies intronic to a long noncoding RNA, *GAPLINC*. Whether these genes prove to be the target genes of these associations has yet to be determined; neither gene has been implicated in endo-

metriosis or ovarian cancer to date. The lead SNPs in these regions displayed strong associations ($p \leq 3.2 \times 10^{-4}$) with endometriosis risk and HGSOE risk in the single trait GWAS datasets and the combined signal achieved genome-wide significance ($p < 5 \times 10^{-8}$). Moreover, GWAS-PW colocalization analysis of each these loci indicated a high probability (≥ 0.76) of a single causal signal underlying the association with both traits.

Different regions shared between endometriosis and different histotypes may suggest possible biological mechanisms driving these causal relationships and the pathways contributing to risk of specific subtypes. Three regions identified as associated with both CCOC and endometriosis using bivariate meta-analysis and GWAS-PW, chromosome 4 near *KDR*, chromosome 8 near *GDAP1*, and chromosome 12 near *VEZT*, were not identified for ENOC and HGSOE. Similarly, genomic regions on chromosome 1 near *DNM3* and chromosome 11 near *FSHB* were associated with ENOC not CCOC or HGSOE, loci on chromosome 9 near *ABO*, and chromosome 10 near *MLLT10* were associated with HGSOE, not CCOC or ENOC. Alternatively, risk variants in the *SKAP1* locus on chromosome 17 were common between endometriosis and most histotypes. Shared variants in regions of known hormone-responsive genes, estrogen-responsive growth regulation by estrogen in breast cancer 1 (*GREB1*)⁵⁰ and kinase insert domain receptor (*KDR*),⁵¹ may suggest a role of hormone regulation in the causal pathway between endometriosis and CCOC. Cell adhesion pathways were also significantly enriched for genes annotated to SNPs associated with risk of endometriosis and CCOC, suggesting that the ability of cells to adhere may contribute to the pathogenesis of endometriosis and subsequently CCOC. Association between variants in the risk loci shared between endometriosis and EOC histotypes and other reproductive traits and diseases, including PCOS, uterine fibroids, and sex hormone levels, suggests that perturbation of underlying pathways important for the development and regulation of the reproductive and endocrine systems may predispose women to a variety of diseases, the development of a particular disease dependent on the presence of additional genetic and environmental risk factors.

Interestingly, the direction of effect at some shared risk loci differed between EOC histotypes. The hepatocyte nuclear factor 1 beta (*HNF1B*) locus showed the same direction of effect between endometriosis and CCOC but was different between endometriosis and HGSOE, consistent with published observations between CCOC and HGSOE.⁵² *HNF1B* is consistently highly expressed in CCOC but the promoter is methylated in HGSOE, suggesting absence of *HNF1B* is critical for development of the HGSOE histotype,^{52,53} potentially against a common background of genetic liability to endometriosis. *HNF1B* is a transcription factor that plays a vital role in tissue development, and regulation of genes involved in cell cycle modulation, apoptosis, oxidative stress response, and epithelial mesenchymal transition, and dysregulation of these pathways may suggest a role for the microenvironment in tumor development.^{54,55} Similarly, SNPs in the *SYNE1* locus on chromosome 6 have the same direction of effect between endometriosis and CCOC but the opposite direction of effect between endometriosis and HGSOE.

We provide evidence of functional mechanisms by which genetic variants associated with these diseases may be affecting

noncoding regulatory elements that control the expression of genes that, when perturbed, increase risk of endometriosis and/or EOC. Overall, many target genes shared between endometriosis and EOC differed between histotypes, supporting evidence from other analyses in this study that different genes and gene pathways may contribute to the causal relationship between endometriosis and the different histotypes. The 1p36.12 risk region was associated with risk of endometriosis, CCOC, ENOC, and HGSOE. *WNT4* lies in this region and is a member of the Wnt/ β -catenin signaling pathway, which has been associated with endometriosis previously.^{56,57} *LINC00339* was also associated with risk of endometriosis and HGSOE at this locus based on the SMR endometrial eQTL analysis. The expression of *LINC00339* and nearby *CDC42* has been associated with endometriosis previously and *LINC00339* has been reported as the likely target gene.^{58,59} Masuda et al.⁶⁰ also report that this same locus on chromosome 1 is associated with risk of both endometriosis and EOC in Japanese women. Methylation at a CpG site near *GREB1* in endometrium and blood is associated with increased risk for endometriosis and CCOC. This association has been identified for endometriosis previously, with functional studies yet to determine the molecular mechanisms contributing to disease risk.^{61,62} Transcription of *GREB1* splice variants has been associated with variants in this region in ovarian tissue.⁶³ This gene is expressed in EOC tumors, with studies suggesting a reliance on *ESR1/GREB1* signaling.^{64,65}

Overlap with chromatin biofeatures in ovarian and endometriosis tissues also highlighted potential target genes. Risk SNPs in the *VEZT* region overlapped the putative bidirectional promoter for *VEZT* and *FGD6*. The lead SNP from the bivariate meta-analysis in the *VEZT* locus (rs7309252) was in LD ($r^2 = 0.99$) with an SNP (rs6538618) overlapping 10 regulatory biofeatures. Expression of both *VEZT* and *FGD6* has been associated with endometriosis risk previously.^{35,58} Similarly, the lead SNPs in the *FSHB* and *MLLT10* loci were in LD ($r^2 > 0.8$) with SNPs overlapping 11 biofeatures in the promoter region of ADP Ribosylation Factor Like GTPase 14 Effector Protein (*ARL14EP*) and *MLLT10* respectively and were associated with methylation at nearby CpG sites. Risk SNPs associated with endometriosis, HGSOE, and LMPSOC span follicle-stimulating hormone (FSH) subunit B (*FSHB*) and nearby *ARL14EP*. *ARL14EP* is expressed by many tissue types and plays a role in the movement of major histocompatibility class II molecules along the actin cytoskeleton. *FSHB* is expressed in the pituitary gland and plays an important role regulating reproductive function. Variants in the 11p14.1 locus near *FSHB* have been significantly associated with multiple reproductive traits and diseases, including PCOS, uterine fibroids, circulating sex hormone levels, and menstrual cycle characteristics.^{17,66–72} The lead SNP from the bivariate meta-analysis, rs11031005, is in LD with a *FSHB* promoter polymorphism (rs10835638) and enhancer polymorphism (rs11031006) involved in regulating *FSHB* transcription.^{73–75} The locus containing the histone lysine methyltransferase DOT1L cofactor (*MLLT10*) was associated with endometriosis risk in a recent endometriosis GWAS.²⁵ Studies have also linked EOC susceptibility and endometriosis risk to subtle variations in regulation at the *MLLT10* promoter

region.^{35,76} SNPs in LD ($r^2 > 0.8$) with the lead variant from the bivariate meta-analysis have been annotated to the promoter of *MLLT10* and have been associated with changes of expression of nearby genes *C10orf140*, *C10orf114*, and *NEBL* in primary EOC tissues and changes in expression of *NEBL* in endometrium, suggesting this promoter may also have cis-regulatory activity across the locus.^{35,76} The emergence of single-cell transcriptomic data in cell types relevant to endometriosis and EOC offer further opportunities to explore potential cell-type-specific effects on candidate genes.^{42–44,77}

ENOC and CCOC are believed to arise from ectopic (endometriosis-derived) or eutopic endometrial epithelium, while HGSOE is presumed to originate from fallopian tube secretory epithelial cells.⁷⁸ Despite the distinct cells of origin, we have previously shown that inherited genetic susceptibility to ENOC/CCOC and HGSOE is, to some extent, shared.⁷⁹ In the current study we find that some risk variants and susceptibility genes for endometriosis, ENOC/CCOC, and HGSOE are also shared and the extent of germline genetic overlap between endometriosis and ENOC/CCOC is much greater than that between endometriosis and HGSOE. Taken together, this supports previous epidemiological associations between endometriosis and ENOC/CCOC, and less stronger epidemiological evidence for an association with HGSOE,¹³ and suggests a model where the shared and non-shared components of genetic predisposition and an underlying background of endometriosis likely interact with cellular context-specific somatic mutational profiles and stromal/hormonal microenvironments to give rise to the distinct histological subtypes of EOC.

In conclusion we found evidence of a strong genetic correlation and causal relationship between endometriosis and two EOC histotypes, CCOC and ENOC, and to a lesser extent with HGSOE. Further investigation into shared genomic regions revealed different genetic variants, genes, and pathways that likely contribute to the causal relationship with the different histotypes. These results add to our understanding of disease pathogenesis and yield genomic targets that may facilitate preventive pharmacological intervention by disrupting the link between endometriosis and EOC and promote targeted EOC screening in women with endometriosis.

Limitations of the study

This study used a comprehensive range of statistical genetic approaches to build on existing evidence of an association between endometriosis and EOC using genetic data from the largest GWAS meta-analyses of endometriosis and EOC risk currently available. The power of this study to identify shared risk loci and target genes is, however, limited by the sample size of some of the less common EOC histotype cohorts, such as LMPSOC. The identification of genetic relationships may also be limited by phenotypic annotation and heterogeneity between endometriosis cases affecting the endometriosis GWAS. Several studies have reported an association between endometriosis sub-phenotypes and risk of EOC, in particular endometriomas.^{5,80–82} More comprehensive phenotyping and molecular characterization of endometriosis lesions could be used to test genetic associations between potential endometriosis subtypes and risk of certain EOC histotypes; for example, testing if the

association between endometriosis and CCOC is driven by endometriomas specifically.

Data from a range of disease-relevant tissues were included in the analyses to provide functional evidence of molecular mechanisms and target genes at risk loci. Further functional evidence and cell-type-specific effects associated with disease risk and subtypes could be explored using additional disease-relevant cell types and single-cell technologies. Target genes identified in this study will require functional validation in appropriate model systems.

Genetic datasets used in this study were restricted to European cohorts and results may not be directly transferable across ancestries.

CONSORTIA

International Endometriosis Genetics Consortium

Yadav Sapkota, Valgerdur Steinthorsdottir, Andrew P. Morris, Amelie Fassbender, Nilufer Rahmioglu, Immaculata De Vivo, Julie E. Buring, Futao Zhang, Todd L. Edwards, Sarah Jones, Dorien O, Daniëlle Peterse, Kathryn M. Rexrode, Paul M. Ridker, Andrew J. Schork, Stuart MacGregor, Nicholas G. Martin, Christian M. Becker, Sosuke Adachi, Kosuke Yoshihara, Takayuki Enomoto, Atsushi Takahashi, Yoichiro Kamatani, Koichi Matsuda, Michiaki Kubo, Gudmar Thorleifsson, Reynir T. Geirsson, Unnur Thorsteinsdottir, Leanne M. Wallace, iPSYCH-SSI-Broad Groupw, Jian Yang, Digna R. Velez Edwards, Mette Nyegaard, Siew-Kee Low, Krina T. Zondervan, Stacey A. Missmer, Thomas D'Hooghe, Grant W. Montgomery, Daniel I. Chasman, Kari Stefansson, Joyce Y. Tung, and Dale R. Nyholt.

Ovarian Cancer Association Consortium

Hoda Anton-Culver, Elisa V. Bandera, Susana N Banerjee, Javier Benitez, Andrew Berchuck, Line Bjorge, Ingrid A. Boere, James D. Brenton, Ralf Butzow, Ian Campbell, Kexin Chen, Georgia Chenevix-Trench, Linda S. Cook, Daniel W. Cramer, Anna de Fazio, Jennifer A. Doherty, Thilo Dörk, Diana M. Eccles, Peter A. Fasching, Renée T. Fortner, Rosalind Glasspool, Ellen L. Goode, Marc T. Goodman, Jacek Gronwald, Claus K. Høgdall, Estrid Høgdall, Chad Hamilton, Holly R. Harris, Florian Heitz, Michelle A.T. Hildebrandt, Akira Hirasawa, Antoinette Hollestelle, David G. Huntsman, Issei Imoto, Beth Y. Karlan, Linda E. Kelemen, Lambertus A. Kiemeny, Susanne K. Kjaer, Anita Koushik, Mieke Kriege, Björg Kristjansdottir, Jolanta Kupryjanczyk, Diether Lambrechts, Nhu D. Le, Douglas A. Levine, Keitaro Matsuo, G Larry Maxwell, Taymaa May, Iain A. McNeish, Usha Menon, Roger L. Milne, Francesmary Modugno, Alvaro N. Monteiro, Patricia G. Moorman, Kirsten B. Moysich, Heli Nevanlinna, Sara H. Olson, Håkan Olsson, Sue K. Park, Celeste L. Pearce, Tanja Pejovic, Malcolm C. Pike, Susan J. Ramus, Elio Riboli, Marjorie J. Riggan, Harvey A. Risch, Cristina Rodriguez-Antona, Isabelle Romieu, Dale P. Sandler, Joellen M. Schildkraut, V. Wendy Setiawan, Kang Shan, Nadeem Siddiqui, Weiva Sieh, Meir Stampfer, Karin Sundfeldt, Rebecca Sutphen, Anthony J. Swerdlow, Soo Hwang Teo, Kathryn L. Terry, Shelley S. Tworoger, Digna Velez Edwards, Roel C.H. Vermeulen, Penelope M. Webb, Nicolas Wentzensen, Emily White, Walter Willett, Alicja Wolk, Yin

Ling Woo, Anna H. Wu, Li Yan, Drakoulis Yannoukakos, Wei Zheng.

STAR★METHODS

Detailed methods are provided in the online version of this paper and include the following:

- **KEY RESOURCES TABLE**
- **RESOURCE AVAILABILITY**
 - Lead contact
 - Materials availability
 - Data and code availability
- **EXPERIMENTAL MODEL AND SUBJECT DETAILS**
 - Primary tissues
- **METHOD DETAILS**
 - Epithelial ovarian cancer dataset
 - Endometriosis dataset
 - H3K27ac ChIP-seq and ATAC-seq
- **QUANTIFICATION AND STATISTICAL ANALYSIS**
 - Genetic correlation and Mendelian randomization
 - Cross-trait meta-analysis
 - Colocalization analyses
 - Gene-based association analysis
 - Functional annotation
 - H3K27ac ChIP-seq and ATAC-seq peak calling
 - Summary-data-based Mendelian randomization (SMR)
 - Expression of target genes

SUPPLEMENTAL INFORMATION

Supplemental information can be found online at <https://doi.org/10.1016/j.xcrm.2022.100542>.

ACKNOWLEDGMENTS

We would like to thank the research participants and employees of 23andMe for making this work possible. We would like to acknowledge the International Endometriosis Genetics Consortium and Ovarian Cancer Association Consortium for their contributions generating the GWAS datasets and data access. We are grateful to the thousands of patients who donated the specimens that enable this research to happen. For specific acknowledgments for the endometriosis meta-analysis, please see Sapkota et al.¹⁷ For specific acknowledgments for the ovarian cancer meta-analysis, please see Phelan et al.¹⁸ The GTEx Project was supported by the Common Fund of the Office of the Director of the National Institutes of Health, and by NCI, NHGRI, NHLBI, NIDA, NIMH, and NINDS. The data used for the analyses described in this manuscript were obtained from the GTEx Portal on 06/26/20.

This work was supported by the National Health and Medical Research Council of Australia (GNT1026033, GNT1105321, GNT1147846, Investigator Grant 1177194 to G.W.M. and Medical Research Future Fund Research grant MRF1199785 to S.M.) and National Institutes of Health (R01CA193910, R01CA204954, R01CA211707, R01CA251555). S.P.K. is supported by a United Kingdom Research and Innovation Future Leaders Fellowship (MR/T043202/1). K.L. is supported by a Liz Tilberis Early Career Award (599175) and a Program Project Development (373356) from the Ovarian Cancer Research Alliance, plus a Research Scholar's Grant from the American Cancer Society (134005). For funding details of the endometriosis meta-analysis, please see Sapkota et al.¹⁷ For funding details of the ovarian cancer meta-analysis, please see Phelan et al.¹⁸

AUTHOR CONTRIBUTIONS

S.M., S.P.K., K.L., G.W.M., and P.P. designed the study with input from the other authors. Data analyzed in this study were generated by the Ovarian Cancer Association Consortium and International Endometriosis Genetics Consortium. S.M. and S.P.K. ran additional quality control and filtering of GWAS datasets. J.-H.S., M.L.F., S.A.G., M.T.S., R.L., C.W., I.C., B.Y.K., P.A.W.R., and B.J.R. contributed to specimen collection and data generation. Data analysis was performed by S.M., S.P.K., R.I.C., and P.F.K., which was interpreted by all authors. S.M., S.P.K., and K.L. drafted the report with input from all other authors. The final manuscript has been critically revised and approved by all authors.

DECLARATION OF INTERESTS

M.L.F. reports other support from Nuscan Diagnostics outside the scope of the submitted work. C.W. reports research funding support from Merck, is a member of the Immunogen advisory board (1/2022), and has been a member of the Genentech advisory board (8/2020). The remaining authors declare no competing interests.

Received: July 11, 2021

Revised: December 13, 2021

Accepted: January 29, 2022

Published: March 15, 2022

REFERENCES

- Treloar, S., Hadfield, R., Montgomery, G., Lambert, A., Wicks, J., Barlow, D.H., O'Connor, D.T., and Kennedy, S. (2002). The international endogene study: a collection of families for genetic research in endometriosis. *Fertil. Sterility* 78, 679–685. [https://doi.org/10.1016/S0015-0282\(02\)03341-1](https://doi.org/10.1016/S0015-0282(02)03341-1).
- Giudice, L.C. (2010). Clinical practice: endometriosis. *New Engl. J. Med.* 362, 2389–2398. <https://doi.org/10.1056/NEJMcp1000274>.
- Rowlands, I.J., Abbott, J.A., Montgomery, G.W., Hockey, R., Rogers, P., and Mishra, G.D. (2021). Prevalence and incidence of endometriosis in Australian women: a data linkage cohort study. *BJOG: Int. J. Obstet. Gynaecol.* 128, 657–665. <https://doi.org/10.1111/1471-0528.16447>.
- American Society for Reproductive, M. (1997). Revised American society for reproductive medicine classification of endometriosis: 1996. *Fertil. Steril.* 67, 817–821. [https://doi.org/10.1016/S0015-0282\(97\)81391-X](https://doi.org/10.1016/S0015-0282(97)81391-X).
- Kok, V.C., Tsai, H.-J., Su, C.-F., and Lee, C.-K. (2015). The risks for ovarian, endometrial, breast, colorectal, and other cancers in women with newly diagnosed endometriosis or adenomyosis: a population-based study. *Int. J. Gynecol. Cancer* 25, 968. <https://doi.org/10.1097/IGC.0000000000000454>.
- Brilhante, A.V.M., Augusto, K.L., Portela, M.C., Sucupira, L.C.G., Oliveira, L.A.F., Pouchaim, A.J.M.V., Nóbrega, L.R.M., Magalhães, T.F.d., and Sobreira, L.R.P. (2017). Endometriosis and ovarian cancer: an integrative review (endometriosis and ovarian cancer). *Asian Pac. J. Cancer Prev.* 18, 11–16. <https://doi.org/10.22034/APJCP.2017.18.1.11>.
- Zafrakas, M., Grimbizis, G., Timologou, A., and Tarlatzis, B.C. (2014). Endometriosis and ovarian cancer risk: a systematic review of epidemiological studies. *Front. Surg.* 1, 14. <https://doi.org/10.3389/fsurg.2014.00014>.
- Anglesio, M.S., Bashashati, A., Wang, Y.K., Senz, J., Ha, G., Yang, W., Aniba, M.R., Prentice, L.M., Farahani, H., Li Chang, H., et al. (2015). Multifocal endometriotic lesions associated with cancer are clonal and carry a high mutation burden. *J. Pathol.* 236, 201–209. <https://doi.org/10.1002/path.4516>.
- Wiegand, K.C., Shah, S.P., Al-Agha, O.M., Zhao, Y., Tse, K., Zeng, T., Senz, J., McConechy, M.K., Anglesio, M.S., Kalloger, S.E., et al. (2010). ARID1A mutations in endometriosis-associated ovarian carcinomas. *New Engl. J. Med.* 363, 1532–1543. <https://doi.org/10.1056/NEJMoa1008433>.
- Jones, S., Wang, T.-L., Shih, I.-M., Mao, T.-L., Nakayama, K., Roden, R., Glas, R., Slamon, D., Diaz, L.A., Vogelstein, B., et al. (2010). Frequent mutations of chromatin remodeling gene ARID1A in ovarian clear cell carcinoma. *Science* 330, 228. <https://doi.org/10.1126/science.1196333>.
- Rossing, M.A., Cushing-Haugen, K.L., Wicklund, K.G., Doherty, J.A., and Weiss, N.S. (2008). Risk of epithelial ovarian cancer in relation to benign ovarian conditions and ovarian surgery. *Cancer Causes Control* 19, 1357. <https://doi.org/10.1007/s10552-008-9207-9>.
- Brinton, L.A., Sakoda, L.C., Sherman, M.E., Frederiksen, K., Kjaer, S.K., Graubard, B.I., Olsen, J.H., and Møller, L. (2005). Relationship of benign gynecologic diseases to subsequent risk of ovarian and uterine tumors. *Cancer Epidemiol. Biomarkers & Prev.* 14, 2929. <https://doi.org/10.1158/1055-9965.EPI-05-0394>.
- Pearce, C.L., Templeman, C., Rossing, M.A., Lee, A., Near, A.M., Webb, P.M., Nagle, C.M., Doherty, J.A., Cushing-Haugen, K.L., Wicklund, K.G., et al. (2012). Association between endometriosis and risk of histological subtypes of ovarian cancer: a pooled analysis of case-control studies. *Lancet Oncol.* 13, 385–394. [https://doi.org/10.1016/s1470-2045\(11\)70404-1](https://doi.org/10.1016/s1470-2045(11)70404-1).
- Vercellini, P., Parazzini, F., Bolis, G., Carinelli, S., Dindelli, M., Vendola, N., Luchini, L., and Crosignani, P.G. (1993). Endometriosis and ovarian cancer. *Am. J. Obstet. Gynecol.* 169, 181–182. [https://doi.org/10.1016/0002-9378\(93\)90159-G](https://doi.org/10.1016/0002-9378(93)90159-G).
- Jimbo, H., Yoshikawa, H., Onda, T., Yasugi, T., Sakamoto, A., and Takeuchi, Y. (1997). Prevalence of ovarian endometriosis in epithelial ovarian cancer. *Int. J. Gynecol. Obstet.* 59, 245–250. [https://doi.org/10.1016/S0020-7292\(97\)00238-5](https://doi.org/10.1016/S0020-7292(97)00238-5).
- Stamp, J.P., Gilks, C.B., Wesseling, M., Eshragh, S., Ceballos, K., Anglesio, M.S., Kwon, J.S., Tone, A., Huntsman, D.G., and Carey, M.S. (2016). BAF250a expression in atypical endometriosis and endometriosis-associated ovarian cancer. *Int. J. Gynecol. Cancer* 26, 825. <https://doi.org/10.1097/IGC.0000000000000698>.
- Sapkota, Y., Steinhorsdottir, V., Morris, A.P., Fassbender, A., Rahmioglu, N., De Vivo, I., Buring, J.E., Zhang, F., Edwards, T.L., Jones, S., et al. (2017). Meta-analysis identifies five novel loci associated with endometriosis highlighting key genes involved in hormone metabolism. *Nat. Commun.* 8, 15539. <https://doi.org/10.1038/ncomms15539>.
- Phelan, C.M., Kuchenbaecker, K.B., Tyrer, J.P., Kar, S.P., Lawrenson, K., Winham, S.J., Dennis, J., Pirie, A., Riggan, M.J., Chornokur, G., et al. (2017). Identification of 12 new susceptibility loci for different histotypes of epithelial ovarian cancer. *Nat. Genet.* 49, 680. <https://doi.org/10.1038/ng.3826>.
- Lu, Y., Cuellar-Partida, G., Painter, J.N., Nyholt, D.R., Australian Ovarian Cancer Study; International Endogene, Consortium; Morris, A.P., Fasching, P.A., Hein, A., Burghaus, S., et al. (2015). Shared genetics underlying epidemiological association between endometriosis and ovarian cancer. *Hum. Mol. Genet.* 24, 5955–5964. <https://doi.org/10.1093/hmg/ddv306>.
- Bulik-Sullivan, B., Finucane, H.K., Anttila, V., Gusev, A., Day, F.R., Loh, P.-R., Duncan, L., Perry, J.R.B., Patterson, N., Robinson, E.B., et al. (2015). An atlas of genetic correlations across human diseases and traits. *Nat. Genet.* 47, 1236–1241. <https://doi.org/10.1038/ng.3406>.
- Ning, Z., Pawitan, Y., and Shen, X. (2020). High-definition likelihood inference of genetic correlations across human complex traits. *Nat. Genet.* 52, 859–864. <https://doi.org/10.1038/s41588-020-0653-y>.
- Burgess, S., Butterworth, A., and Thompson, S.G. (2013). Mendelian randomization analysis with multiple genetic variants using summarized data. *Genet. Epidemiol.* 37, 658–665. <https://doi.org/10.1002/gepi.21758>.
- Bowden, J., Davey Smith, G., Haycock, P.C., and Burgess, S. (2016). Consistent estimation in mendelian randomization with some invalid instruments using a weighted median estimator. *Genet. Epidemiol.* 40, 304–314. <https://doi.org/10.1002/gepi.21965>.
- Bowden, J., Davey Smith, G., and Burgess, S. (2015). Mendelian randomization with invalid instruments: effect estimation and bias detection

- through Egger regression. *Int. J. Epidemiol.* **44**, 512–525. <https://doi.org/10.1093/ije/dyv080>.
25. Rahmioglu, N., Banasik, K., Christofidou, P., Danning, R., Galarneau, G., Giri, A., MacGregor, S., Mortlock, S., Sapkota, Y., Schork, A.J., et al. (2018). Large-scale genome-wide association meta-analysis of endometriosis reveals 13 novel loci and genetically-associated comorbidity with other pain conditions. *bioRxiv*. Preprint at. <https://doi.org/10.1101/406967>.
 26. Verbanck, M., Chen, C.Y., Neale, B., and Do, R. (2018). Detection of widespread horizontal pleiotropy in causal relationships inferred from Mendelian randomization between complex traits and diseases. *Nat. Genet.* **50**, 693–698. <https://doi.org/10.1038/s41588-018-0099-7>.
 27. Trochet, H., Pirinen, M., Band, G., Jostins, L., McVean, G., and Spencer, C.C.A. (2019). Bayesian meta-analysis across genome-wide association studies of diverse phenotypes. *Genet. Epidemiol.* **43**, 532–547. <https://doi.org/10.1002/gepi.22202>.
 28. Han, B., and Eskin, E. (2011). Random-effects model aimed at discovering associations in meta-analysis of genome-wide association studies. *Am. J. Hum. Genet.* **88**, 586–598. <https://doi.org/10.1016/j.ajhg.2011.04.014>.
 29. Lee, C.H., Eskin, E., and Han, B. (2017). Increasing the power of meta-analysis of genome-wide association studies to detect heterogeneous effects. *Bioinformatics* **33**, i379–i388. <https://doi.org/10.1093/bioinformatics/btx242>.
 30. Pickrell, J.K., Berisa, T., Liu, J.Z., Séguirel, L., Tung, J.Y., and Hinds, D.A. (2016). Detection and interpretation of shared genetic influences on 42 human traits. *Nat. Genet.* **48**, 709–717. <https://doi.org/10.1038/ng.3570>.
 31. Bakshi, A., Zhu, Z., Vinkhuyzen, A.A.E., Hill, W.D., McRae, A.F., Visscher, P.M., and Yang, J. (2016). Fast set-based association analysis using summary data from GWAS identifies novel gene loci for human complex traits. *Sci. Rep.* **6**, 32894. <https://doi.org/10.1038/srep32894>.
 32. Liao, Y., Wang, J., Jaehning, E.J., Shi, Z., and Zhang, B. (2019). WebGestalt 2019: gene set analysis toolkit with revamped UIs and APIs. *Nucleic Acids Res.* **47**, W199–W205. <https://doi.org/10.1093/nar/gkz401>.
 33. Corona, R.I., Seo, J.-H., Lin, X., Hazelett, D.J., Reddy, J., Fonseca, M.A.S., Abassi, F., Lin, Y.G., Mhawech-Fauceglia, P.Y., Shah, S.P., et al. (2020). Non-coding somatic mutations converge on the PAX8 pathway in ovarian cancer. *Nat. Commun.* **11**, 2020. <https://doi.org/10.1038/s41467-020-15951-0>.
 34. Coetzee, S.G., Shen, H.C., Hazelett, D.J., Lawrenson, K., Kuchenbaecker, K., Tyrer, J., Rhie, S.K., Levanon, K., Karst, A., Drapkin, R., et al. (2015). Cell-type-specific enrichment of risk-associated regulatory elements at ovarian cancer susceptibility loci. *Hum. Mol. Genet.* **24**, 3595–3607. <https://doi.org/10.1093/hmg/ddv101>.
 35. Mortlock, S., Kendarsari, R.I., Fung, J.N., Gibson, G., Yang, F., Restuadi, R., Girling, J.E., Holdsworth-Carson, S.J., Teh, W.T., Lukowski, S.W., et al. (2020). Tissue specific regulation of transcription in endometrium and association with disease. *Hum. Reprod.* **35**, 377–393. <https://doi.org/10.1093/humrep/dez279>.
 36. Consortium, G., Aguet, F., Brown, A.A., Castel, S.E., Davis, J.R., He, Y., Jo, B., Mohammadi, P., Park, Y., Parsana, P., et al. (2017). Genetic effects on gene expression across human tissues. *Nature* **550**, 204. <https://doi.org/10.1038/nature24277>. <https://www.nature.com/articles/nature24277#supplementary-information>.
 37. Watanabe, K., Taskesen, E., van Bochoven, A., and Posthuma, D. (2017). Functional mapping and annotation of genetic associations with FUMA. *Nat. Commun.* **8**, 1826. <https://doi.org/10.1038/s41467-017-01261-5>.
 38. Zhu, Z., Zhang, F., Hu, H., Bakshi, A., Robinson, M.R., Powell, J.E., Montgomery, G.W., Goddard, M.E., Wray, N.R., Visscher, P.M., and Yang, J. (2016). Integration of summary data from GWAS and eQTL studies predicts complex trait gene targets. *Nat. Genet.* **48**, 481–487. <https://doi.org/10.1038/ng.3538>. <http://www.nature.com/ng/journal/v48/n5/abs/ng.3538.html#supplementary-information>.
 39. Fung, J.N., Girling, J.E., Lukowski, S.W., Sapkota, Y., Wallace, L., Holdsworth-Carson, S.J., Henders, A.K., Healey, M., Rogers, P.A.W., Powell, J.E., and Montgomery, G.W. (2017). The genetic regulation of transcription in human endometrial tissue. *Hum. Reprod.* **32**, 893–904. <https://doi.org/10.1093/humrep/dex006>.
 40. Vösa, U., Claringbould, A., Westra, H.-J., Bonder, M.J., Deelen, P., Zeng, B., Kirsten, H., Saha, A., Kreuzhuber, R., Yazar, S., et al. (2021). Large-scale cis- and trans-eQTL analyses identify thousands of genetic loci and polygenic scores that regulate blood gene expression. *Nat. Genet.* **53**, 1300–1310. <https://doi.org/10.1038/s41588-021-00913-z>.
 41. McRae, A.F., Marioni, R.E., Shah, S., Yang, J., Powell, J.E., Harris, S.E., Gibson, J., Henders, A.K., Bowdler, L., Painter, J.N., et al. (2018). Identification of 55,000 replicated DNA methylation QTL. *Scientific Rep.* **8**, 17605. <https://doi.org/10.1038/s41598-018-35871-w>.
 42. Wang, W., Vilella, F., Alama, P., Moreno, I., Mignardi, M., Isakova, A., Pan, W., Simon, C., and Quake, S.R. (2020). Single-cell transcriptomic atlas of the human endometrium during the menstrual cycle. *Nat. Med.* **26**, 1644–1653. <https://doi.org/10.1038/s41591-020-1040-z>.
 43. Ma, J., Zhang, L., Zhan, H., Mo, Y., Ren, Z., Shao, A., and Lin, J. (2021). Single-cell transcriptomic analysis of endometriosis provides insights into fibroblast fates and immune cell heterogeneity. *Cell Biosci.* **11**, 125. <https://doi.org/10.1186/s13578-021-00637-x>.
 44. Liu, Z., Sun, Z., Liu, H., Niu, W., Wang, X., Liang, N., Wang, X., Wang, Y., Shi, Y., Xu, L., and Shi, W. (2021). Single-cell transcriptomic analysis of eutopic endometrium and ectopic lesions of adenomyosis. *Cell Biosci.* **11**, 51. <https://doi.org/10.1186/s13578-021-00562-z>.
 45. Wei, J.-J., William, J., and Bulun, S. (2011). Endometriosis and ovarian cancer: a review of clinical, pathologic, and molecular aspects. *Int. J. Gynecol. Pathol.* **30**, 553–568. <https://doi.org/10.1097/PGP.0b013e31821f4b85>.
 46. Lee, A.W., Templeman, C., Stram, D.A., Beesley, J., Tyrer, J., Berchuck, A., Pharoah, P.P., Chenevix-Trench, G., Pearce, C.L., and Ovarian Cancer Association, C. (2016). Evidence of a genetic link between endometriosis and ovarian cancer. *Fertil. Steril.* **105**, 35–43.e1–10. <https://doi.org/10.1016/j.fertnstert.2015.09.023>.
 47. Yarmolinsky, J., Relton, C.L., Lophatananon, A., Muir, K., Menon, U., Gentry-Maharaj, A., Walther, A., Zheng, J., Fasching, P., Zheng, W., et al. (2019). Appraising the role of previously reported risk factors in epithelial ovarian cancer risk: a Mendelian randomization analysis. *PLoS Med* **16**, e1002893. <https://doi.org/10.1371/journal.pmed.1002893>.
 48. Duffy, D.L., Zhu, G., Li, X., Sanna, M., Iles, M.M., Jacobs, L.C., Evans, D.M., Yazar, S., Beesley, J., Law, M.H., et al. (2018). Novel pleiotropic risk loci for melanoma and nevus density implicate multiple biological pathways. *Nat. Commun.* **9**, 4774. <https://doi.org/10.1038/s41467-018-06649-5>.
 49. An, J., Gharahkhani, P., Law, M.H., Ong, J.S., Han, X., Olsen, C.M., Neale, R.E., Lai, J., Vaughan, T.L., Gockel, I., et al. (2019). Gastroesophageal reflux GWAS identifies risk loci that also associate with subsequent severe esophageal diseases. *Nat. Commun.* **10**, 4219. <https://doi.org/10.1038/s41467-019-11968-2>.
 50. Mohammed, H., D’Santos, C., Serandour, A.A., Ali, H.R., Brown, Gordon D., Atkins, A., Rueda, Oscar M., Holmes, K.A., Theodorou, V., Robinson, J.L.L., et al. (2013). Endogenous purification reveals GREB1 as a key estrogen receptor regulatory factor. *Cell Rep.* **3**, 342–349. <https://doi.org/10.1016/j.celrep.2013.01.010>.
 51. Sugino, N., Kashida, S., Karube-Harada, A., Takiguchi, S., and Kato, H. (2002). Expression of vascular endothelial growth factor (VEGF) and its receptors in human endometrium throughout the menstrual cycle and in early pregnancy. *Reproduction* **123**, 379–387. <https://doi.org/10.1530/rep.0.1230379>.
 52. Natanzon, Y., Goode, E.L., and Cunningham, J.M. (2018). Epigenetics in ovarian cancer. *Semin. Cancer Biol.* **51**, 160–169. <https://doi.org/10.1016/j.semcancer.2017.08.003>.
 53. Ross-Adams, H., Ball, S., Lawrenson, K., Halim, S., Russell, R., Wells, C., Strand, S.H., Ørntoft, T.F., Larson, M., Armasu, S., et al. (2016). HNF1B

- variants associate with promoter methylation and regulate gene networks activated in prostate and ovarian cancer. *Oncotarget* 7, 74734–74746. <https://doi.org/10.18632/oncotarget.12543>.
54. Suzuki, E., Kajita, S., Takahashi, H., Matsumoto, T., Tsuruta, T., and Saegusa, M. (2015). Transcriptional upregulation of HNF-1 β by NF- κ B in ovarian clear cell carcinoma modulates susceptibility to apoptosis through alteration in bcl-2 expression. *Lab. Invest.* 95, 962–972. <https://doi.org/10.1038/labinvest.2015.73>.
 55. Yamaguchi, K., Amano, Y., Matsumura, N., Mandai, M., Abiko, K., Hamanishi, J., Yoshioka, Y., Baba, T., and Konishi, I. (2014). *HNF1B* contributes to resistance to oxidative stress through modification of metabolism in ovarian clear cell carcinoma. *Gynecol. Oncol.* 133, 87. <https://doi.org/10.1016/j.ygyno.2014.03.232>.
 56. Pazhohan, A., Amidi, F., Akbari-Asbagh, F., Seyedrezazadeh, E., Farzadi, L., Khodarahmin, M., Mehdinejadani, S., and Sobhani, A. (2018). The Wnt/ β -catenin signaling in endometriosis, the expression of total and active forms of β -catenin, total and inactive forms of glycogen synthase kinase-3 β , WNT7a and DICKKOPF-1. *Eur. J. Obstet. Gynecol. Reprod. Biol.* 220, 1–5. <https://doi.org/10.1016/j.ejogrb.2017.10.025>.
 57. Matsuzaki, S., Botchorishvili, R., Pouly, J.L., and Canis, M. (2014). Targeting the Wnt/ β -catenin pathway in endometriosis: a potentially effective approach for treatment and prevention. *Mol. Cell Ther.* 2, 36. <https://doi.org/10.1186/s40591-014-0036-9>.
 58. Fung, J.N., Mortlock, S., Girling, J.E., Holdsworth-Carson, S.J., Teh, W.T., Zhu, Z., Lukowski, S.W., McKinnon, B.D., McRae, A., Yang, J., et al. (2018). Genetic regulation of disease risk and endometrial gene expression highlights potential target genes for endometriosis and polycystic ovarian syndrome. *Scientific Rep.* 8, 11424. <https://doi.org/10.1038/s41598-018-29462-y>.
 59. Powell, J.E., Fung, J.N., Shakhbazov, K., Sapkota, Y., Cloonan, N., Heman, G., Hillman, K.M., Kaufmann, S., Luong, H.T., Bowdler, L., et al. (2016). Endometriosis risk alleles at 1p36.12 act through inverse regulation of CDC42 and LINC00339. *Hum. Mol. Genet.* 25, 5046–5058. <https://doi.org/10.1093/hmg/ddw320>.
 60. Masuda, T., Low, S.-K., Akiyama, M., Hirata, M., Ueda, Y., Matsuda, K., Kimura, T., Murakami, Y., Kubo, M., Kamatani, Y., and Okada, Y. (2019). GWAS of five gynecologic diseases and cross-trait analysis in Japanese. *Eur. J. Hum. Genet.* 28, 95–107. <https://doi.org/10.1038/s41431-019-0495-1>.
 61. Mortlock, S., Restuadi, R., Levien, R., Girling, J.E., Holdsworth-Carson, S.J., Healey, M., Zhu, Z., Qi, T., Wu, Y., Lukowski, S.W., et al. (2019). Genetic regulation of methylation in human endometrium and blood and gene targets for reproductive diseases. *Clin. Epigenet.* 11, 49. <https://doi.org/10.1186/s13148-019-0648-7>.
 62. Fung, J.N., Holdsworth-Carson, S.J., Sapkota, Y., Zhao, Z.Z., Jones, L., Girling, J.E., Paiva, P., Healey, M., Nyholt, D.R., Rogers, P.A.W., and Montgomery, G.W. (2015). Functional evaluation of genetic variants associated with endometriosis near GREB1. *Hum. Reprod.* 30, 1263–1275. <https://doi.org/10.1093/humrep/dev051>.
 63. The GTEx Consortium atlas of genetic regulatory effects across human tissues. *Science* 369, 1318. <https://doi.org/10.1126/science.aaz1776>.
 64. Hodgkinson, K., Forrest, L.A., Vuong, N., Garson, K., Djordjevic, B., and Vanderhyden, B.C. (2018). GREB1 is an estrogen receptor-regulated tumour promoter that is frequently expressed in ovarian cancer. *Oncogene* 37, 5873–5886. <https://doi.org/10.1038/s41388-018-0377-y>.
 65. Laviolette, L.A., Hodgkinson, K.M., Minhas, N., Perez-Iratxeta, C., and Vanderhyden, B.C. (2014). 17 β -estradiol upregulates GREB1 and accelerates ovarian tumor progression in vivo. *Int. J. Cancer* 135, 1072–1084. <https://doi.org/10.1002/ijc.28741>.
 66. Day, F., Karaderi, T., Jones, M.R., Meun, C., He, C., Drong, A., Kraft, P., Lin, N., Huang, H., Broer, L., et al. (2018). Large-scale genome-wide meta-analysis of polycystic ovary syndrome suggests shared genetic architecture for different diagnosis criteria. *PLoS Genet.* 14, e1007813. <https://doi.org/10.1371/journal.pgen.1007813>.
 67. Day, F.R., Ruth, K.S., Thompson, D.J., Lunetta, K.L., Pervjakova, N., Chasman, D.I., Stolk, L., Finucane, H.K., Sulem, P., Bulik-Sullivan, B., et al. (2015). Large-scale genomic analyses link reproductive aging to hypothalamic signaling, breast cancer susceptibility and BRCA1-mediated DNA repair. *Nat. Genet.* 47, 1294. <https://doi.org/10.1038/ng.3412>. <https://www.nature.com/articles/ng.3412#supplementary-information>.
 68. Day, F.R., Thompson, D.J., Helgason, H., Chasman, D.I., Finucane, H., Sulem, P., Ruth, K.S., Whalen, S., Sarkar, A.K., Albrecht, E., et al. (2017). Genomic analyses identify hundreds of variants associated with age at menarche and support a role for puberty timing in cancer risk. *Nat. Genet.* 49, 834. <https://doi.org/10.1038/ng.3841>. <https://www.nature.com/articles/ng.3841#supplementary-information>.
 69. Gallagher, C.S., Mäkinen, N., Harris, H.R., Rahmioglu, N., Uimari, O., Cook, J.P., Shiges, N., Ferreira, T., Velez-Edwards, D.R., Edwards, T.L., et al. (2019). Genome-wide association and epidemiological analyses reveal common genetic origins between uterine leiomyomata and endometriosis. *Nat. Commun.* 10, 4857. <https://doi.org/10.1038/s41467-019-12536-4>.
 70. Laisk, T., Kukuškina, V., Palmer, D., Laber, S., Chen, C.-Y., Ferreira, T., Rahmioglu, N., Zondervan, K., Becker, C., Smoller, J.W., et al. (2018). Large-scale meta-analysis highlights the hypothalamic–pituitary–gonadal axis in the genetic regulation of menstrual cycle length. *Hum. Mol. Genet.* 27, 4323–4332. <https://doi.org/10.1093/hmg/ddy317>.
 71. Mbarek, H., Steinberg, S., Nyholt, D.R., Gordon, S.D., Miller, M.B., McRae, A.F., Hottenga, J.J., Day, F.R., Willemsen, G., de Geus, E.J., et al. (2016). Identification of common genetic variants influencing spontaneous dizygotic twinning and female fertility. *Am. J. Hum. Genet.* 98, 898–908. <https://doi.org/10.1016/j.ajhg.2016.03.008>.
 72. Ruth, K.S., Campbell, P.J., Chew, S., Lim, E.M., Hadlow, N., Stuckey, B.G.A., Brown, S.J., Feenstra, B., Joseph, J., Surdulescu, G.L., et al. (2016). Genome-wide association study with 1000 genomes imputation identifies signals for nine sex hormone-related phenotypes. *Eur. J. Hum. Genet.* 24, 284–290. <https://doi.org/10.1038/ejhg.2015.102>.
 73. Grigорова, M., Punab, M., Ausmees, K., and Laan, M. (2008). FSHB promoter polymorphism within evolutionary conserved element is associated with serum FSH level in men. *Hum. Reprod.* 23, 2160–2166. <https://doi.org/10.1093/humrep/den216>.
 74. Trevisan, C.M., de Oliveira, R., Christofolini, D.M., Barbosa, C.P., and Bianco, B. (2019). Effects of a polymorphism in the promoter region of the follicle-stimulating hormone subunit beta (FSHB) gene on female reproductive outcomes. *Genet. Test Mol. Biomarkers* 23, 39–44. <https://doi.org/10.1089/gtmb.2018.0182>.
 75. Bohaczuk, S.C., Thackray, V.G., Shen, J., Skowronska-Krawczyk, D., and Mellon, P.L. (2021). FSHB transcription is regulated by a novel 5' distal enhancer with a fertility-associated single nucleotide polymorphism. *Endocrinology* 162, bqaa181. <https://doi.org/10.1210/endo/bqaa181>.
 76. Pharoah, P.D.P., Tsai, Y.-Y., Ramus, S.J., Phelan, C.M., Goode, E.L., Lawrenson, K., Buckley, M., Fridley, B.L., Tyrer, J.P., Shen, H., et al. (2013). GWAS meta-analysis and replication identifies three new susceptibility loci for ovarian cancer. *Nat. Genet.* 45, 362–370. <https://doi.org/10.1038/ng.2564>.
 77. Dinh, H.Q., Lin, X., Abbasi, F., Nameki, R., Haro, M., Olingy, C.E., Chang, H., Hernandez, L., Gayther, S.A., Wright, K.N., et al. (2021). Single-cell transcriptomics identifies gene expression networks driving differentiation and tumorigenesis in the human fallopian tube. *Cell Rep.* 35, 108978. <https://doi.org/10.1016/j.celrep.2021.108978>.
 78. Cochrane, D.R., Tessier-Cloutier, B., Lawrence, K.M., Nazeran, T., Karnezis, A.N., Salamanca, C., Cheng, A.S., McAlpine, J.N., Hoang, L.N., Gilks, C.B., and Huntsman, D.G. (2017). Clear cell and endometrioid carcinomas: are their differences attributable to distinct cells of origin? *J. Pathol.* 243, 26–36. <https://doi.org/10.1002/path.4934>.
 79. Cuellar-Partida, G., Lu, Y., Dixon, S.C., Fasching, P.A., Hein, A., Burghaus, S., Beckmann, M.W., Lambrechts, D., Van Nieuwenhuysen, E., Vergote, I., et al. (2016). Assessing the genetic architecture of epithelial ovarian cancer

- histological subtypes. *Hum. Genet.* *135*, 741–756. <https://doi.org/10.1007/s00439-016-1663-9>.
80. Kobayashi, H., Sumimoto, K., Moniwa, N., Imai, M., Takakura, K., Kuro-maki, T., Morioka, E., Arisawa, K., and Terao, T. (2007). Risk of developing ovarian cancer among women with ovarian endometrioma: a cohort study in Shizuoka, Japan. *Int. J. Gynecol. Cancer* *17*, 37–43. <https://doi.org/10.1111/j.1525-1438.2006.00754.x>.
81. Buis, C.C., van Leeuwen, F.E., Mooij, T.M., and Burger, C.W. (2013). Increased risk for ovarian cancer and borderline ovarian tumours in subfertile women with endometriosis. *Hum. Reprod. (Oxford, England)* *28*, 3358–3369. <https://doi.org/10.1093/humrep/det340>.
82. Saavalainen, L., Lassus, H., But, A., Tiitinen, A., Härkki, P., Gissler, M., Pukkala, E., and Heikinheimo, O. (2018). Risk of gynecologic cancer according to the type of endometriosis. *Obstet. Gynecol.* *131*, 1095–1102. <https://doi.org/10.1097/aog.0000000000002624>.
83. Gu, Z., Eils, R., and Schlesner, M. (2016). Complex heatmaps reveal patterns and correlations in multidimensional genomic data. *Bioinformatics* *32*, 2847–2849. <https://doi.org/10.1093/bioinformatics/btw313>.
84. Jones, M.R., Peng, P.C., Coetzee, S.G., Tyrer, J., Reyes, A.L.P., Corona, R.I., Davis, B., Chen, S., Dezem, F., Seo, J.H., et al. (2020). Ovarian cancer risk variants are enriched in histotype-specific enhancers and disrupt transcription factor binding sites. *Am. J. Hum. Genet.* *107*, 622–635. <https://doi.org/10.1016/j.ajhg.2020.08.021>.
85. Karst, A.M., and Drapkin, R. (2012). Primary culture and immortalization of human fallopian tube secretory epithelial cells. *Nat. Protoc.* *7*, 1755–1764. <https://doi.org/10.1038/nprot.2012.097>.
86. Fotheringham, S., Levanon, K., and Drapkin, R. (2011). Ex vivo culture of primary human fallopian tube epithelial cells. *J. Vis. Exp.* *51*, 2728. <https://doi.org/10.3791/2728>.
87. Yavorska, O.O., and Burgess, S. (2017). MendelianRandomization: an R package for performing Mendelian randomization analyses using summarized data. *Int. J. Epidemiol.* *46*, 1734–1739. <https://doi.org/10.1093/ije/dyx034>.
88. Berisa, T., and Pickrell, J.K. (2015). Approximately independent linkage disequilibrium blocks in human populations. *Bioinformatics* *32*, 283–285. <https://doi.org/10.1093/bioinformatics/btv546>.
89. Giambartolomei, C., Vukcevic, D., Schadt, E.E., Franke, L., Hingorani, A.D., Wallace, C., and Plagnol, V. (2014). Bayesian test for colocalisation between pairs of genetic association studies using summary statistics. *PLoS Genet.* *10*, e1004383. <https://doi.org/10.1371/journal.pgen.1004383>.

STAR★METHODS

KEY RESOURCES TABLE

REAGENT or RESOURCE	SOURCE	IDENTIFIER
Deposited data		
EOC GWA Meta-analysis Summary Statistics	Ovarian Cancer Association Consortium Phelan et al. ¹⁸	http://ocac.ccge.medschl.cam.ac.uk/
Endometrial eQTL summary statistics	Fung et al. ³⁹	http://reproductivegenomics.com.au/shiny/endo_eqtl_rna/
	Mortlock et al. ³⁵	http://reproductivegenomics.com.au/shiny/eeqtl2/
eQTLGen Blood eQTLs summary statistics	Võsa et al. ⁴⁰	https://www.eqtlgen.org/
GTEx eQTL summary statistics	Consortium et al. ³⁶	https://www.gtexportal.org/home/
H3K27ac ChIP-seq data	Corona et al. ³³	GEO:GSE68104
	Coetzee et al. ³⁴	GEO:GSE121103
	This study	GEO:GSE197928
ATAC-seq data	This study	GEO:GSE197928
Single-cell RNA-seq	Wang et al. ⁴²	GEO:GSE111976
Software and algorithms		
LDSC	Bulik-Sullivan et al. ²⁰	https://github.com/bulik/ldsc
HDL	Ning et al. ²¹	https://github.com/zhenin/HDL
Mendelian Randomization (MR)	R package MendelianRandomization version 0.5.0	https://cran.r-project.org/web/packages/MendelianRandomization/index.html
MR-PRESSO	Verbanck et al. ²⁶	https://github.com/rondolab/MR-PRESSO
MetABF	Trochet et al. ²⁷	https://github.com/trochet/metabf
RE2C	Lee et al. ²⁹	https://github.com/cuelee/RE2C
GWAS-pw	Pickrell et al. ³⁰	https://github.com/joepickrell/gwas-pw
fastBAT	GCTA	https://cnsgenomics.com/software/gcta/#Overview
	Bakshi et al. ³¹	
Over-representation analysis	WebGestalt	http://www.webgestalt.org/
	Liao et al. ³²	
GENE2FUNC	FUMA	https://fuma.ctglab.nl/
	Watanabe et al. ³⁷	
Peak Calling	ENCODE pipeline (v1.2.2)	https://www.encodeproject.org/pipelines/
Summary-data-based Mendelian Randomization (SMR)	Zhu et al. ³⁸	https://cnsgenomics.com/software/smr/#Overview
ComplexHeatmap	Gu et al. ⁸³	https://bioconductor.org/packages/release/bioc/html/ComplexHeatmap.html
Other		
Endometriosis GWA Meta-analysis Summary Statistics	International Endometriosis Genetics Consortium Sapkota et al. ¹⁷	N/A

RESOURCE AVAILABILITY

Lead contact

Further information and requests for resources should be directed to and will be fulfilled by the lead contact, Dr Sally Mortlock (s.mortlock@imb.uq.edu.au).

Materials availability

This study did not generate new unique reagents.

Data and code availability

Endometrioma H3K27ac ChIP-seq data and ATAC-seq data have been deposited at Gene Expression Omnibus (GEO) and are publicly available as of the date of publication. Accession numbers are listed in the [key resources table](#). This paper also analyses existing, publicly available data. These accession numbers for the datasets are listed in the key resources table. This paper does not report original code. Any additional information required to reanalyse the data reported in this paper is available from the lead contact upon request.

EXPERIMENTAL MODEL AND SUBJECT DETAILS

Primary tissues

ChIP-seq and ATAC-seq data were generated for primary tissues (ChIP-seq - endometriosis (endometrioma) and adjacent endometriosis-associated stroma; ATAC-seq - fallopian tube and clear cell and high-grade serous ovarian cancer tissues) collected, with informed consent, as part of the Gynecologic Tissue Bank at Cedars-Sinai Medical Center or at the University of Southern California. Tissues were OCT embedded and H&Es reviewed to confirm the diagnosis.

METHOD DETAILS

Epithelial ovarian cancer dataset

Genetic data in the form of GWAS summary statistics were available from a 2017 GWAS meta-analysis for EOC and EOC histotypes conducted by Phelan et al.¹⁸ Summary statistics included the SNP RSID, effect allele, other allele, effect allele frequency, beta coefficient (be), standard error (SE) and p-value. The meta-analysis included 25,509 EOC cases and 40,941 controls of European ancestry with association statistics reported for 10,197,379 SNPs for overall EOC, high-grade serous ovarian cancer (HGSOC) (n = 13,037), low-grade serous ovarian cancer (LGSOC) (n = 1,012), low malignant potential serous ovarian cancer (LMPsOC) (n = 1,954), mucinous ovarian cancer (MOC) (n = 1,417), endometrioid ovarian cancer (ENOC) (n = 2,810) and clear cell ovarian cancer (CCOC) (n = 1,366). Summary statistics were filtered to remove SNPs with an imputation quality r^2 (OncoArray) score <0.3 and SNPs with a minor allele frequency (MAF) < 0.01 leaving 10,197,379 SNPs for subsequent analysis.

Endometriosis dataset

Endometriosis GWAS summary statistics were available from the 2017 GWAS meta-analysis for endometriosis conducted by Sapkota et al.¹⁷ Summary statistics include the SNP RSID, effect allele, other allele, beta coefficient (be), standard error (SE), effect allele frequency, and p-value. Only statistics generated from European cohorts was used in subsequent analyses including 14,949 cases and 190,715 controls. Summary statistics for 7,899,415 SNPs remained following removal of imputed genotypes with low imputation quality (<0.3 for minimac and <0.4 for IMPUTE2) and SNPs with a MAF <0.01.

H3K27ac ChIP-seq and ATAC-seq

ChIP-seq - H3K27ac ChIP-seq data have been previously described^{33,34,84} with the exception of the primary endometrioma and endometrioma stroma specimens, which were profiled in parallel with the tumors reported in Corona et al.³³ 5mm punch biopsies were taken from frozen tissue blocks, and were pulverized using the Covaris CryoPrep system (Covaris, Woburn, MA), then fixed using 1% formaldehyde (Thermo fisher, Waltham, MA) diluted in Phosphate-buffered saline solution (10 min at room temperature) and quenched with 125 mM glycine (10 min at room temperature). Cells were lysed in ice cold lysis buffer (50 mM Tris, 10 mM EDTA, 1% SDS with protease inhibitor; 10 min) and rinsed with ice-cold phosphate-buffered saline solution. The Covaris E210 sonicator was used to shear chromatin to 300–500 base pairs (AFA: 5% duty cycle, 5 intensity, 200 cycles/burst; 10 min). Chromatin samples were diluted with 5 vol of dilution buffer (1% Triton X-100, 2 mM EDTA, 150 mM NaCl, 20 mM Tris-HCl pH 8.1) and incubated overnight at 4°C with 1 μg H3K27ac antibody (DiAGenode, C15410196, Denville, NJ; as a ratio of 1:600) coupled with protein A and protein G beads (Life Technologies, Carlsbad, CA). Chromatin samples were washed five times with RIPA washing buffer (0.05 M HEPES pH 7.6, 1 mM EDTA, 0.7% Na deoxycholate, 1% NP-40, 0.5 M LiCl), once with TE buffer (pH 8.0) and were resuspended in elution buffer (50 mM Tris, 10 mM EDTA, 1% SDS). Samples were treated with RNase (30 min at 37°C) and incubated overnight with proteinase K (65°C). DNA was isolated using the Qiagen Qiaquick kit, and libraries prepared using the ThruPLEX-FD Prep Kit (Rubicon Genomics, Ann Arbor, MI). Sequencing was performed using 75-base pair single reads on the Illumina platform (Illumina, San Diego, CA) at the Dana-Farber Cancer Institute.

ATAC-seq - Epithelial-rich regions of flash frozen tumors were biopsied using a 5mm biopsy punch. Primary fallopian tube tissues were subjected to enzymatic digest using Pronase and DNase1 for 48–72 hours^{85,86} and the epithelial-enriched cells viably frozen down in 10% DMSO/90% fetal bovine serum. In one instance, fallopian epithelial cells were cultured on collagen-coated plates prior to profiling. ATAC-seq was performed by Active Motif, using paired end 42bp reads, and sequenced to a depth of ~40M reads.

QUANTIFICATION AND STATISTICAL ANALYSIS

Genetic correlation and Mendelian randomization

Linkage disequilibrium score regression (LDSC)²⁰ and high-definition likelihood inference (HDL)²¹ was used to estimate the genetic correlation between endometriosis and ovarian cancer histotypes using the GWAS summary statistics. LD scores were computed

using 1000 Genomes European ancestry data as the independent variable in the LD Score regression and for the regression weights. In the absence of sample overlap between the datasets we also constrained the LD score regression intercept to reduce the standard error substantially. Mendelian randomization (MR) analyses were performed using the R package MendelianRandomization version 0.5.0.⁸⁷ Inverse-variance weighted (IVW)²² regression was used for primary analysis and weighted median²³ and MR-Egger regression²⁴ for sensitivity analyses with models that are more robust to horizontal pleiotropy. Associations were declared significant if both IVW and weighted median analyses yielded P-values < 0.05 and the direction of the effect size estimates (odds ratios) were consistent across IVW, weighted median, MR-Egger regression approaches. Of the 27 independent, genome-wide significant (P-value < 5x10⁻⁸) endometriosis lead risk SNPs,²⁵ two multiallelic SNPs (rs484686 and rs4762173) were removed, leaving 25 SNPs in the instrument for genetic liability to endometriosis. Further, we also used the MR-PRESSO “global test”²⁶ and the MR-Egger intercept test²⁴ to detect statistical evidence of horizontal pleiotropy and if the MR-PRESSO global test found such evidence it was followed by outlier (pleiotropic) SNP removal and the MR-PRESSO “distortion test” to identify potential distortion of the MR estimate after outlier SNP removal. Finally, we also tested for reverse-directional causal effects using MR by evaluating the association between genetic liability to EOC histotypes and endometriosis risk. Where fewer than three genome-wide significant (P-value < 5x10⁻⁸) SNPs were available to instrument a EOC histotype (for CCOC, ENOC and LGSOC) we used SNPs associated with that histotype at P-value < 10⁻⁵ to enable application of the primary IVW MR method in the EOC to endometriosis direction.

Cross-trait meta-analysis

To identify risk loci associated with both traits we conducted a bivariate meta-analysis using two different approaches, MetABF²⁷ and Han and Eskin random-effects model (RE2C).^{28,29} MetABF is a method to meta-analyse genome-wide association studies using approximate Bayes Factors. Beta coefficients (effect sizes) and SEs from the endometriosis dataset were used as input for MetABF alongside beta coefficients and SEs from ovarian cancer histotypes. Each of the six ovarian cancer histotypes were meta-analysed with endometriosis separately. Correlation in effect sizes was modeled using both an independent and fixed effect model and the prior parameter for the variance in effect sizes, sigma, was set to 0.1 allowing effect sizes to be small, characteristic of complex diseases. Significantly associated SNPs were defined by log₁₀ ABF >4 in either the fixed or independent model and at least nominal significance in the single trait GWAS (P-value < 0.05).

To validate results, we also performed a routine fixed effects meta-analysis and a modified random effects meta-analysis on the same data using RE2C. RE2C is designed to integrate the effects while accounting for the heterogeneity between studies. A SNP was deemed significantly associated with both traits in the bivariate meta-analysis if it met a fixed (Cochran’s Q statistic P-value > 0.05) or random (Cochran’s Q statistics’s P-value < 0.05) effect threshold of P-value < 5x10⁻⁸ and was at least nominally significant in the single trait GWAS meta-analysis (P-value < 0.05) and had no significant heterogeneity. SNPs found to be significantly associated with both traits and passing thresholds for both MetABF and RE2C were fine mapped using FUMA³⁷ to identify independent signals to identify independent signals at $r^2 < 0.6$.

Colocalization analyses

GWAS-pw³⁰ was used to estimate the probability that in a given genomic region the same variant underlies the association with both traits. The genome is split into 1703 non-overlapping regions using linkage disequilibrium blocks⁸⁸ and following Giambartolomei et al.⁸⁹ the software estimates the probability, using an empirical Bayes approach, that a given genomic region either 1) contains a genetic variant that influences the first trait, 2) contains a genetic variant that influences the second trait, 3) contains a genetic variant that influences both traits (posterior probability of association, PPA3), or 4) contains both a genetic variant that influences the first trait and a separate genetic variant that influences the second trait (PPA4). This was performed using the endometriosis dataset and each ovarian cancer histotype. Regions with a PPA3/4 > 0.5 were considered to have evidence of a shared causal variant and independent causal variants respectively.

Gene-based association analysis

The fastBAT function in GCTA³¹ was used to perform a gene-based association analysis for endometriosis and each ovarian cancer histotype using GWAS summary statistics from each trait. A total of 20,439 genes (hg19) were tested for each disease using an LD cutoff of 0.9 and no SNPs outside defined gene boundaries. Genes in the top 1% and 5% associated with each EOC histotype that overlapped with the top 1% and 5% of genes associated with endometriosis were tested for enrichment in pathways using over-representation analysis in WebGestat.³²

Functional annotation

The GENE2FUNC option in FUMA³⁷ was also used to investigate the expression of nearby (within 10kb) genes across tissues and enrichment of functional and biological pathways.

H3K27ac ChIP-seq and ATAC-seq peak calling

Peak calling of H3K27ac ChIP-seq profiles was performed using the ENCODE pipeline (v1.2.2) with p-val_thresh = 1e-09, reference genome hg38 and other default parameters. If two technical replicates were used, we selected the overlap peak set of the true replicates (rep1_rep2.overlap.bfilt.narrowPeak.gz) as the ‘sample peak set’, otherwise, we used the overlap peak set of the pseudo

replicates (rep1-pr.overlap.bfilt.narrowPeak.gz). Quality control metrics (number of unique mapped reads, cross-correlation metrics, IDR) were checked for each technical replicate (Table S5).

Donor peak set

Two or more sample peak sets are combined if they belong to the same donor, resulting in a set of non-overlapping peaks. First, individual peak scores ($-\log_{10}(\text{p-value})$) are normalized to a 'score per million' (SPM) dividing the peak score, by the sum of all peak scores within the sample, divided by a factor of a million. Then, all peaks from the same donor are merged and sorted by SPM. Iteratively, a peak is removed if it overlaps another peak with a higher SPM, resulting in a set of non-overlapping peaks that represent a donor.

Consensus peak set

A set of sample/donor peak sets will be combined when they are part of the same experiment, tissue type and sample type triage. Similarly to the donor peak set procedure, peaks are merged, sorted and iteratively removed, based on the SPM. Then, the remaining non-overlapping peaks are tagged as reproducible if they overlap peaks with an SPM > 5 in two or more samples. Non-reproducible peaks, peaks that are within repeat mask regions and peaks in the "Y" chromosome are removed, leaving a set of reproducible non-overlapping peaks as the 'consensus peak set'. Consensus peak sets are then transformed from hg38 to hg19 using *liftOver* with parameters `-bedPlus=6`, the `hg38toHg19.over.chain.gz` from UCSC chain files and other default parameters. On average, each consensus peak set has 125.2 (0.28%) genomic locations that could not be mapped (range = [8,350]).

Summary-data-based Mendelian randomization (SMR)

Summary-data-based Mendelian randomization (SMR) is used to assess the association between genetic variants, gene expression/methylation level and risk of disease.³⁸ SMR has been conducted using summary statistics from Sapkota et al.¹⁷ and endometrial and blood eQTLs and mQTLs.^{35,39,41,61} Using these published results, we searched for any significant SMR associations in loci associated ($\log_{10} \text{ABF} > 4$ in the cross-trait MetABF analysis, $P\text{-value} < 5 \times 10^{-8}$ in the cross-trait RE2C analysis and $P\text{-value} < 0.05$ in each single trait meta-analysis) with both endometriosis and ovarian cancer from the bivariate meta-analysis. We also conducted SMR on each ovarian cancer histotype by integrating the GWAS meta-analysis summary data from Phelan et al.¹⁸ and summary eQTL data from endometrium,^{35,39} eQTLGen⁴⁰ and GTEx ovary and uterus.³⁶ Associations were considered significant if they had a $P_{\text{SMR}} < 0.05$ /(number of genes tested) and a $P_{\text{HEIDI}} > 0.05$ /(number of genes passing the SMR test). Of note, associations with $P_{\text{SMR}} < 0.05$ and a $P_{\text{HEIDI}} > 0.05$ were also considered due to power limitations in existing datasets. In the absence of multiple testing correction these would require future validation in larger datasets or functional studies. The heterogeneity in dependent instruments (HEIDI) test³⁸ considers the pattern of risk associations using all the SNPs that are significantly associated with gene expression in a region and evaluates the null hypothesis that there is a single association signal affecting gene expression/methylation and disease risk and the alternative hypothesis that there are distinct variants associated with expression/methylation and disease. Results were filtered to only report those in regions with evidence of a variant associated with both endometriosis and a EOC histotype ($\text{PPA} > 0.5$) as determined by the colocalization analysis.

Expression of target genes

The expression of target genes annotated in the cross-trait meta-analysis, and those identified using fastBAT and SMR, was investigated in eight endometrial cell types using single-cell expression data from Wang et al.⁴² Counts were downloaded from Gene Expression Omnibus (GEO) under accession number GSE111976. Heatmaps for the single-cell expression data were generated using the ComplexHeatmap package⁸³ in R. Counts from both the 10x dataset, generated using the 10x Chromium system, and C1 dataset, generated using Fluidigm C1 medium chips, were plotted.

Cell Reports Medicine, Volume 3

Supplemental information

**A multi-level investigation of the genetic
relationship between endometriosis
and ovarian cancer histotypes**

Sally Mortlock, Rosario I. Corona, Pik Fang Kho, Paul Pharoah, Ji-Heui Seo, Matthew L. Freedman, Simon A. Gayther, Matthew T. Siedhoff, Peter A.W. Rogers, Ronald Leuchter, Christine S. Walsh, Ilana Cass, Beth Y. Karlan, B.J. Rimel, Ovarian Cancer Association Consortium, International Endometriosis Genetics Consortium, Grant W. Montgomery, Kate Lawrenson, and Siddhartha P. Kar

Supplementary Figures

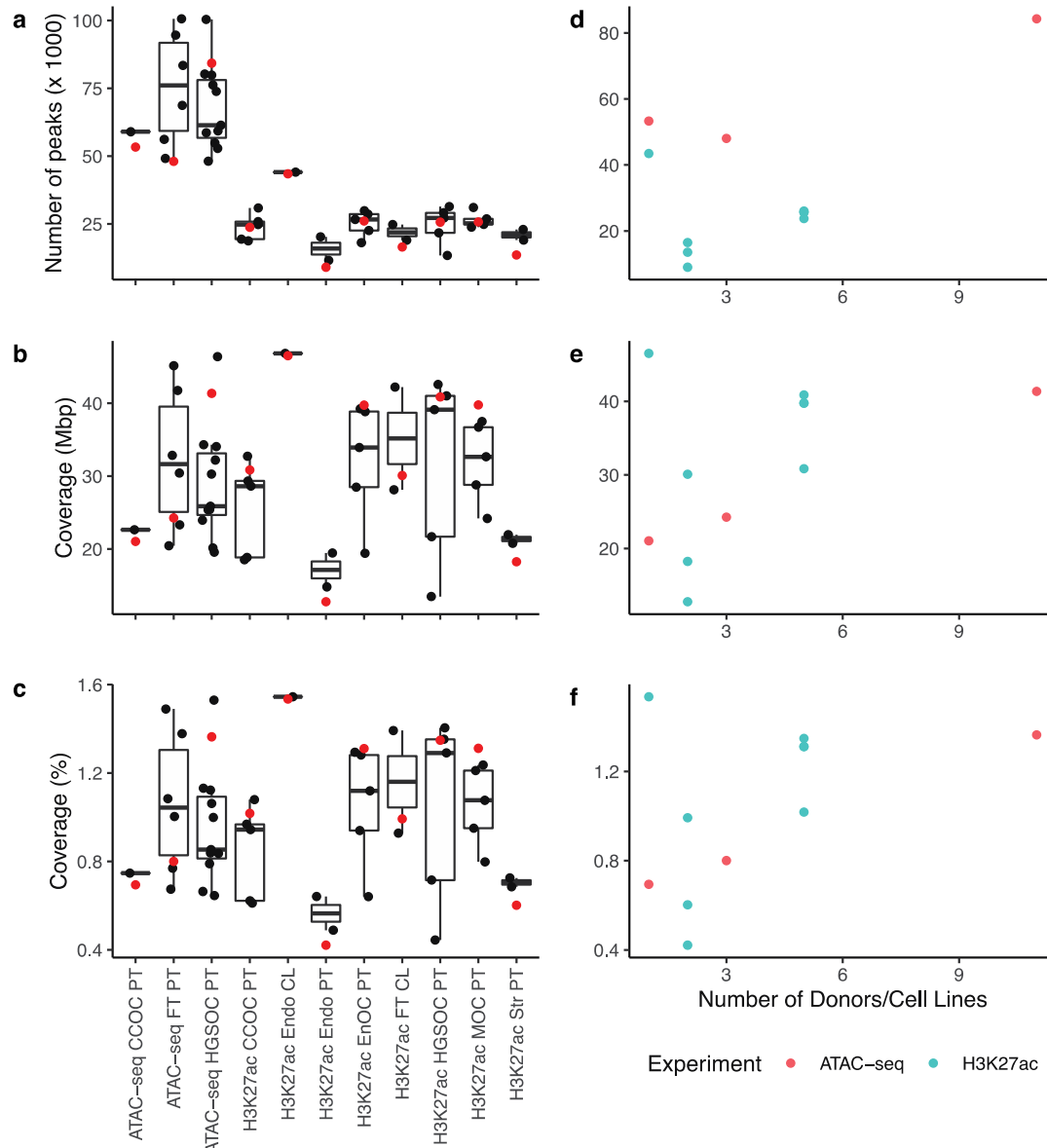


Figure S1. ATAC-seq and H3K27ac CHIP-seq coverage and peaks. (a) Number of peaks and (b) genome coverage in Mbp and (c) genome coverage in percentage for sample peak sets (black dots) and consensus peak sets (red dots). (d) Number of peaks (e) and genome coverage in Mbp and (g) genome coverage in percentage for consensus peak sets as a function of the number of donors. Endo, endometriosis; FT, fallopian tube; Str, endometriosis-associated stroma; CCOC, clear cell ovarian cancer; EnOC, endometrioid ovarian cancer; HGSOC, high-grade serous ovarian cancer; MOC, mucinous ovarian cancer. Data for both primary tissues (PT) and cell lines (CL) is shown. Related to STAR Methods and Table S5.

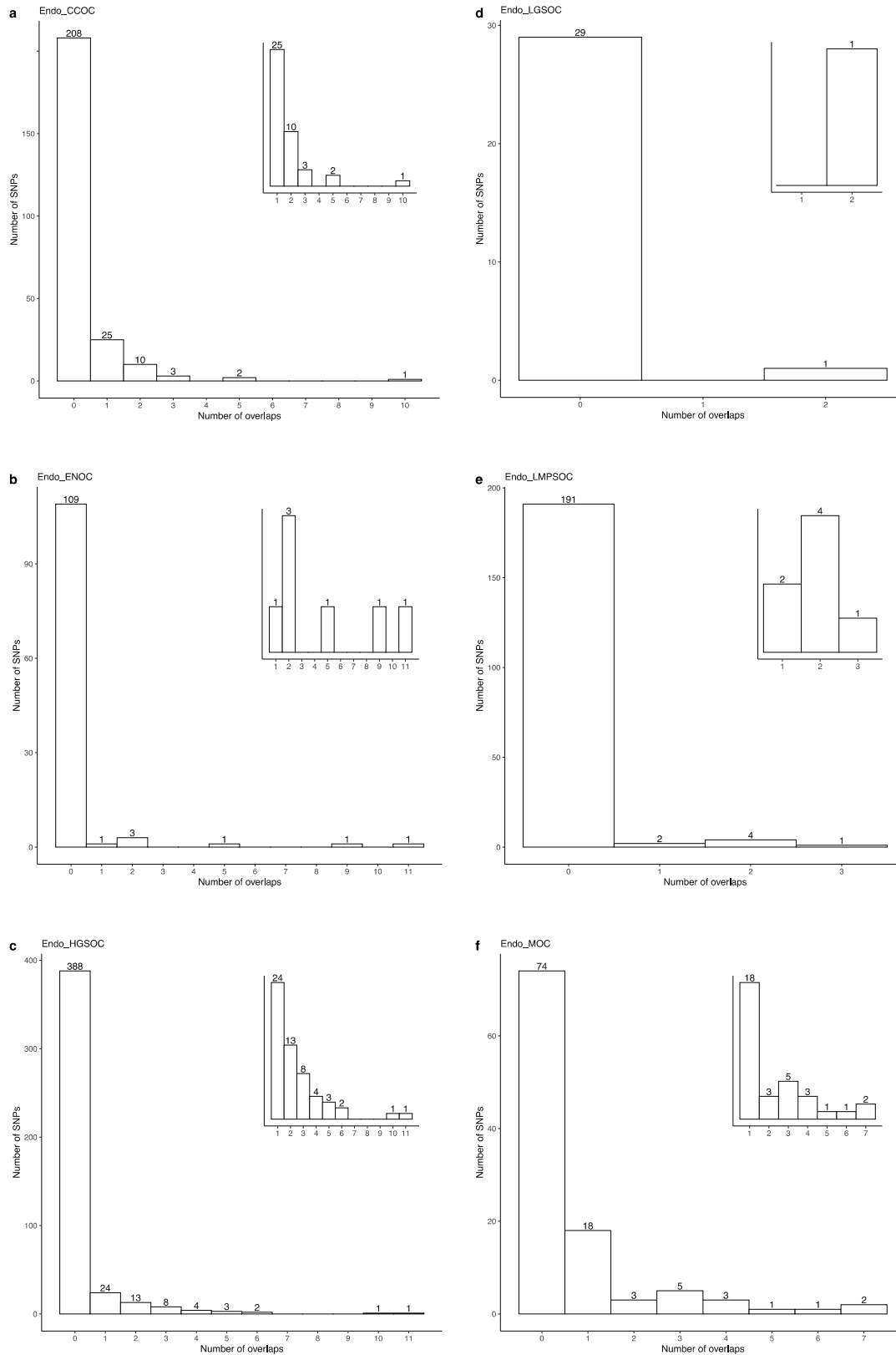


Figure S2. Associated SNPs overlap biofeatures. Histogram of number of SNPs associated with endometriosis and (a) clear cell ovarian cancer (CCOC), (b) endometrioid ovarian cancer (ENOC), (c) high-grade serous ovarian cancer (HGSOC), (d) Low-grade serous ovarian cancer (LGSOC), (e) low malignant potential serous ovarian cancer (LMPSOC) and (f) mucinous ovarian cancer (MOC), that overlap n biofeatures. Inset histograms show the number of overlaps ≥ 1 . Related to Figure 1 and Table S7.

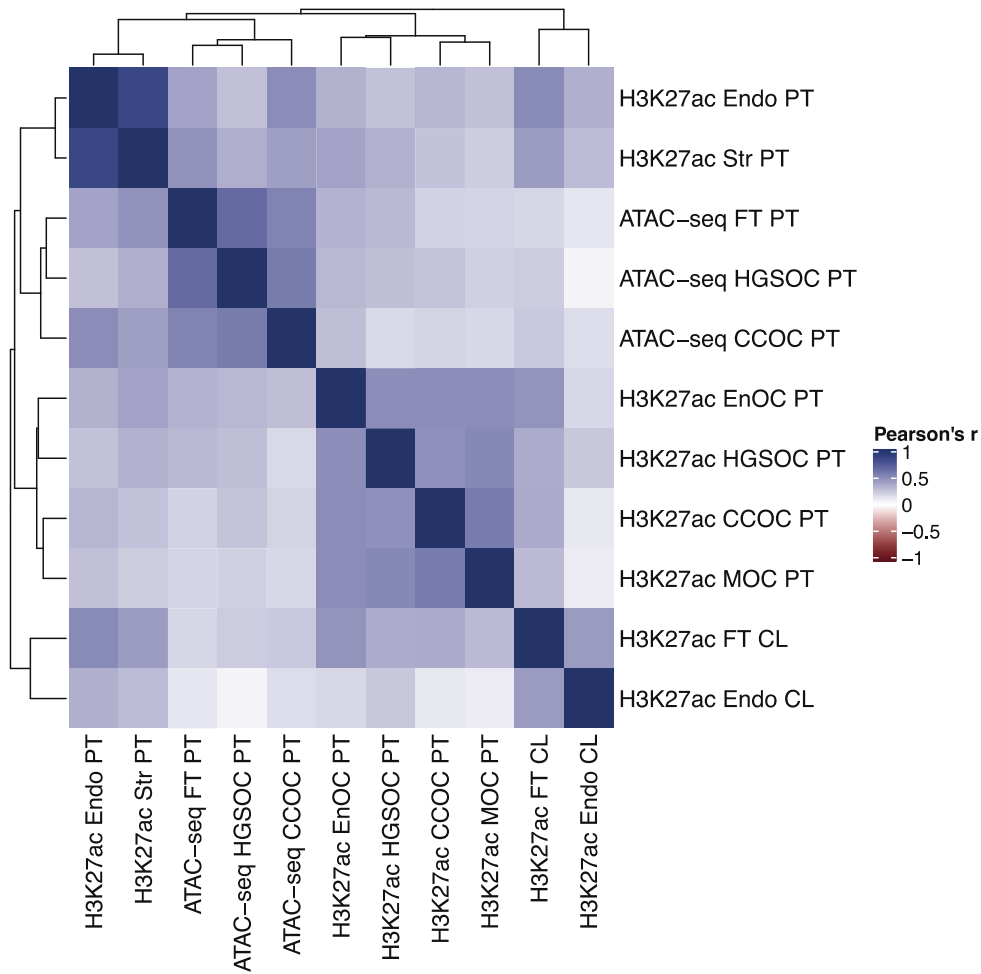


Figure S3. Correlation between biofeature overlap. Pearson's correlation coefficient between ATAC-seq and H3K27ac ChIP-seq biofeatures based on the overlap with SNPs associated with both endometriosis and ovarian cancer risk. Endo, endometriosis; FT, fallopian tube; Str, endometriosis-associated stroma; CCOC, clear cell ovarian cancer; EnOC, endometrioid ovarian cancer; HGSOC, high-grade serous ovarian cancer; MOC, mucinous ovarian cancer. Data for both primary tissues (PT) and cell lines (CL) is shown. Related to Figure 1 and Table S5.

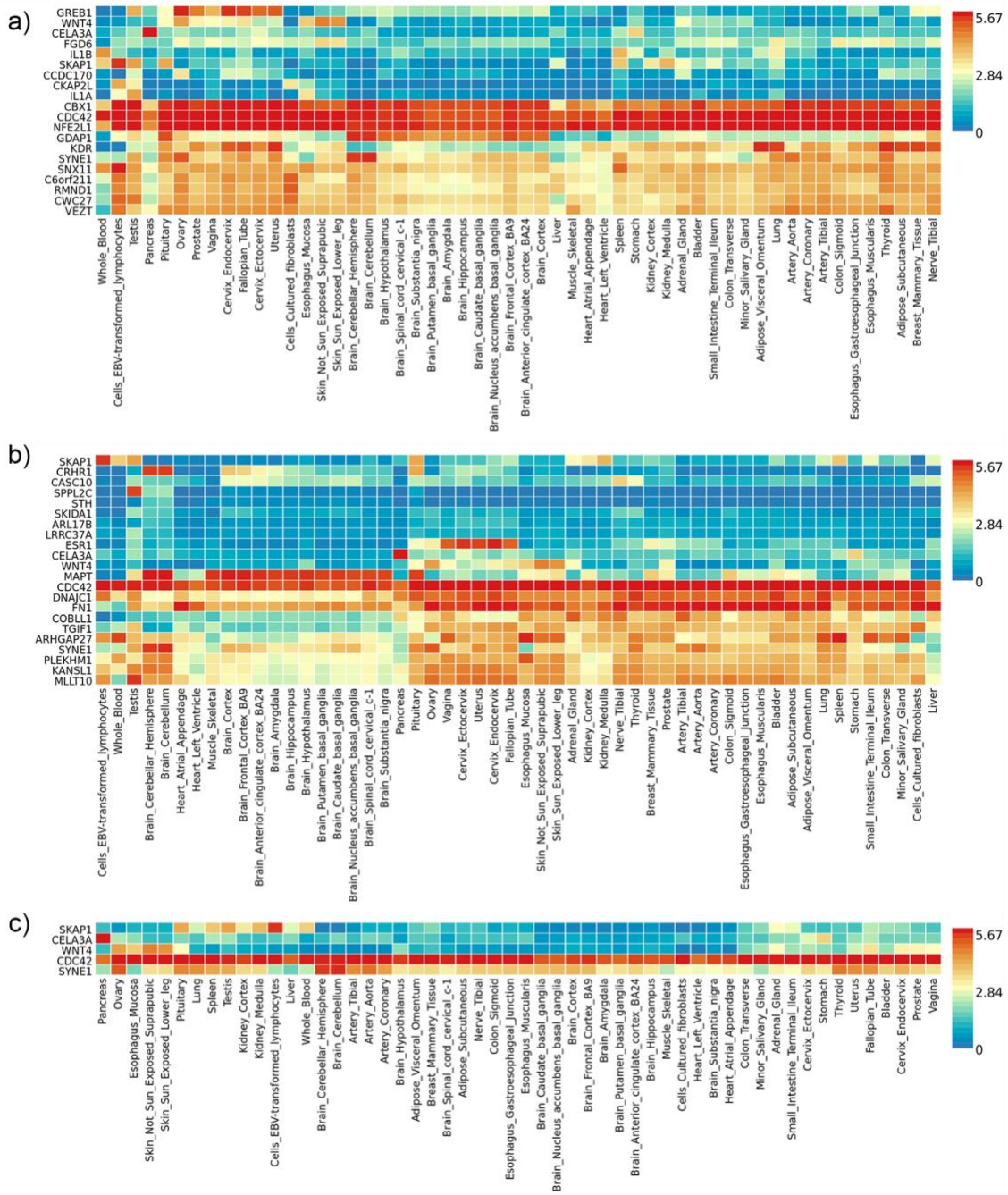


Figure S4. Expression of genes annotated to associated regions. Heatmap, generated in FUMA, of genes annotated to SNPs significantly associated with endometriosis plus (a) clear cell ovarian cancer, (b) high-grade serous ovarian cancer and (c) all three, expressed across 58 tissues from GTEx. Related to Tables 3 and 4 and Table S8.

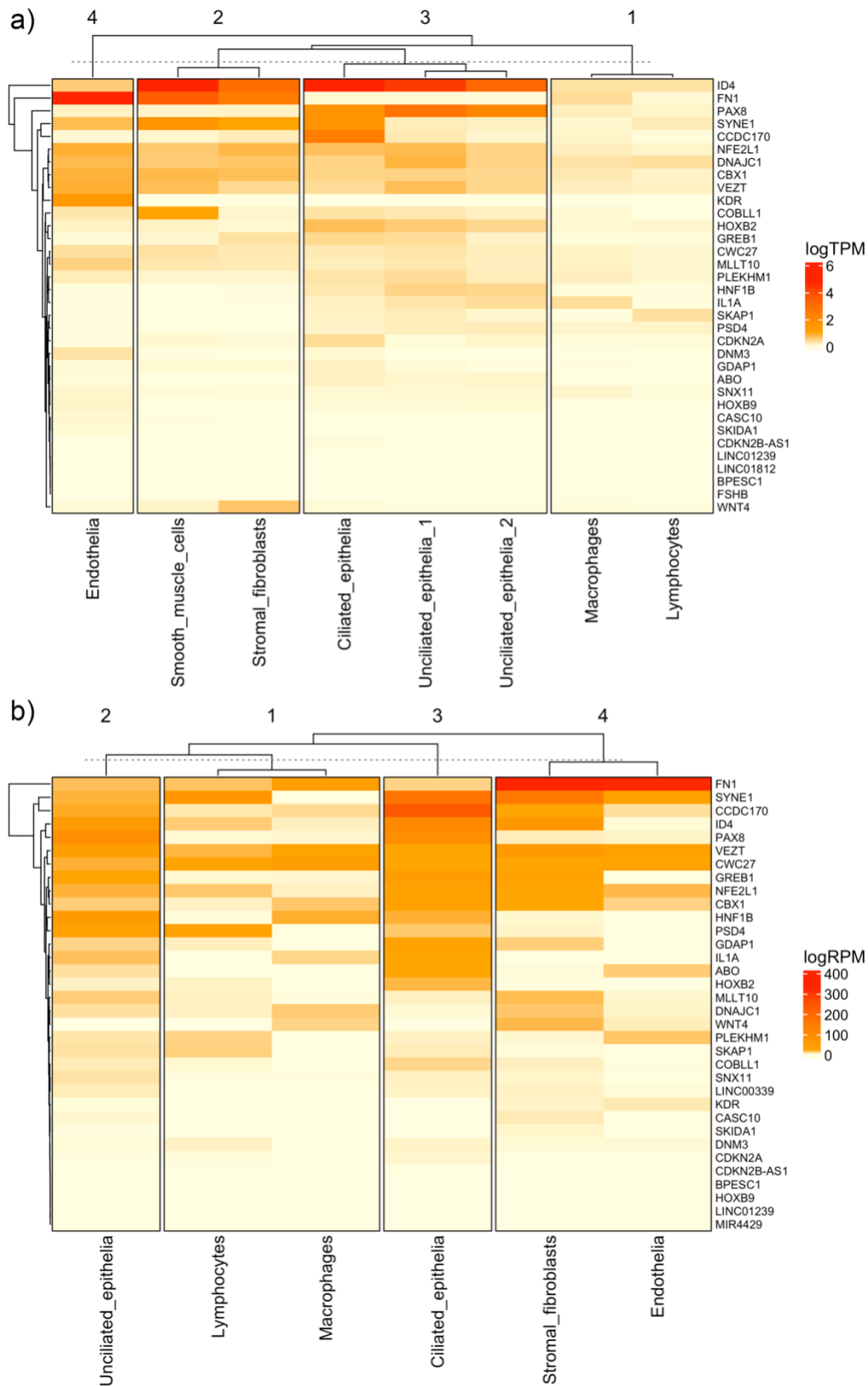


Figure S5. Endometrial single-cell expression of target genes. Heatmaps showing the expression of target genes in eight cell types identified from single-cell sequencing of endometrial samples by Wang et al. 2020 [GSE111976]. Counts from both the 10x dataset (a), generated using the 10x Chromium system, and C1 dataset (b), generated using Fluidigm C1 medium chips, were plotted. Related to Tables 4 and 6.

Supplementary Tables

Table S1. Mendelian Randomization results for the association between genetic liability to each epithelial ovarian cancer (EOC) histotype and endometriosis risk. Related to Table 2. The primary IVW analysis results are in bold font.

Exposure	Method	nsnp	pval	OR	OR_lci95	OR_uci95
Using genetic variants associated with each EOC histotype at P < 5e-8						
High-grade Serous	Inverse variance weighted	14	0.59	1.03	0.93	1.14
High-grade Serous	MR Egger	14	0.64	0.95	0.75	1.19
High-grade Serous	Weighted median	14	0.95	1.00	0.92	1.08
Low Malignant Potential Serous	Inverse variance weighted	3	0.31	1.04	0.97	1.11
Low Malignant Potential Serous	MR Egger	3	0.95	1.01	0.78	1.31
Low Malignant Potential Serous	Weighted median	3	0.52	1.03	0.95	1.11
Mucinous	Inverse variance weighted	4	0.06	1.09	1.00	1.20
Mucinous	MR Egger	4	0.14	7.35	1.37	39.31
Mucinous	Weighted median	4	0.01	1.12	1.03	1.21
Using genetic variants associated with each EOC histotype at P < 1e-5 (because no variants were associated with endometrioid and Low-grade serous EOC risks at P < 5e-8 and only one variant was associated with clear cell EOC risk at P < 5e-8 in our data set, precluding the use of IVW, weighted median and MR-Egger methods, all of which require at least three variants in the genetic instrument for MR)						
Clear Cell	Inverse variance weighted	21	0.41	1.01	0.98	1.05
Clear Cell	MR Egger	21	0.16	1.06	0.98	1.14
Clear Cell	Weighted median	21	0.14	1.03	0.99	1.08
Endometrioid	Inverse variance weighted	11	0.17	0.95	0.88	1.02
Endometrioid	MR Egger	11	0.75	1.04	0.82	1.32
Endometrioid	Weighted median	11	0.75	0.98	0.89	1.08
Low-grade Serous	Inverse variance weighted	26	0.68	0.99	0.97	1.02
Low-grade Serous	MR Egger	26	0.39	0.98	0.92	1.03
Low-grade Serous	Weighted median	26	0.72	0.99	0.96	1.03
nsnp: number of SNPs included as instruments pval: Mendelian Randomisation P-value OR: odds ratio OR_lci95: lower 95% confidence interval odds ratio OR_uci95: upper 95% confidence interval odds ratio						

Table S7. Index SNPs for independent loci from the cross-trait meta-analysis containing SNPs intersecting with biofeatures. Related to Figure 1 and Figure S2.

Comparison	rsID	Chr	Position (bp)	Nearest gene or gene with functional evidence	nOverlap = 0	nOverlap > 0	nOverlap > 0 (%)	Total SNPs
High-grade Serous + Endometriosis	rs7217120	chr17	46484755	<i>SKAPI</i>	220	26	10.57	246
Mucinous + Endometriosis	rs4849174	chr2	113973467	<i>PAX8</i>	42	26	38.24	68
Clear Cell + Endometriosis	rs10167914	chr2	113563361	<i>ILIA</i>	18	12	40.00	30
Clear Cell + Endometriosis	rs11674184	chr2	11721535	<i>GREB1</i>	50	12	19.35	62
High-grade Serous + Endometriosis	rs12037376	chr1	22462111	<i>LINC00339</i>	36	9	20.00	45
High-grade Serous + Endometriosis	rs7084454	chr10	21821274	<i>MLLT10</i>	85	7	7.61	92
High-grade Serous + Endometriosis	rs11658063	chr17	36103872	<i>HNF1B</i>	6	6	50.00	12
Mucinous + Endometriosis	rs11674184	chr2	11721535	<i>GREB1</i>	23	5	17.86	28
Clear Cell + Endometriosis	rs11651755	chr17	36099840	<i>HNF1B</i>	2	4	66.67	6
Clear Cell + Endometriosis	rs12700667	chr7	25901639	<i>AK057379</i>	9	4	30.77	13
Endometrioid + Endometriosis	rs10445377	chr17	46214168	<i>SKAPI</i>	60	4	6.25	64
High-grade Serous + Endometriosis	rs7570979	chr2	11717429	<i>GREB1</i>	17	4	19.05	21
LMP Serous + Endometriosis	rs10445377	chr17	46214168	<i>SKAPI</i>	61	4	6.15	65
Clear Cell + Endometriosis	rs61768001	chr1	22465820	<i>LINC00339</i>	20	3	13.04	23
LMP Serous + Endometriosis	rs35713035	chr17	46501710	<i>SKAPI</i>	119	3	2.46	122
Clear Cell + Endometriosis	rs4516787	chr4	56010165	<i>KDR</i>	74	2	2.63	76
Endometrioid + Endometriosis	rs11031005	chr11	30226356	<i>FSHB</i>	27	2	6.90	29
Mucinous + Endometriosis	rs10167914	chr2	113563361	<i>ILIA</i>	4	2	33.33	6
Clear Cell + Endometriosis	rs1971256	chr6	151816011	<i>CCDC170</i>	0	1	100.00	1
Clear Cell + Endometriosis	rs1311245	chr5	64272107	<i>CWC27</i>	1	1	50.00	2
Clear Cell + Endometriosis	rs7309252	chr12	95687497	<i>VEZT</i>	6	1	14.29	7
Clear Cell + Endometriosis	rs8069263	chr17	46286778	<i>SKAPI</i>	8	1	11.11	9
Endometrioid + Endometriosis	rs1971256	chr6	151816011	<i>CCDC170</i>	5	1	16.67	6
High-grade Serous + Endometriosis	rs1250244	chr2	216297796	<i>FN1</i>	0	1	100.00	1
High-grade Serous + Endometriosis	rs10048393	chr18	3476253	<i>AX721193</i>	2	1	33.33	3

High-grade Serous + Endometriosis	rs111610638	chr6	152449994	<i>SYNE1</i>	4	1	20.00	5
High-grade Serous + Endometriosis	rs635634	chr9	136155000	<i>ABO</i>	9	1	10.00	10
Low-grade Serous + Endometriosis	rs10445377	chr17	46214168	<i>SKAP1</i>	27	1	3.57	28
Clear Cell + Endometriosis	rs17803970	chr6	152553718	<i>SYNE1</i>	9	0	0.00	9
Clear Cell + Endometriosis	rs71575922	chr6	152554014	<i>SYNE1</i>	6	0	0.00	6
Clear Cell + Endometriosis	rs566679	chr9	22634893	<i>LINC01239</i>	3	0	0.00	3
Clear Cell + Endometriosis	rs78103255	chr8	75311331	<i>GDAP1</i>	2	0	0.00	2
Endometrioid + Endometriosis	rs56318008	chr1	22470407	<i>LINC00339</i>	10	0	0.00	10
Endometrioid + Endometriosis	rs6475610	chr9	22141894	<i>CDKN2B-AS1</i>	5	0	0.00	5
Endometrioid + Endometriosis	rs495590	chr1	172122809	<i>DNM3</i>	2	0	0.00	2
High-grade Serous + Endometriosis	rs6908034	chr6	19773930	<i>ID4</i>	3	0	0.00	3
High-grade Serous + Endometriosis	rs62065444	chr17	43565599	<i>PLEKHM1</i>	3	0	0.00	3
High-grade Serous + Endometriosis	rs1981046	chr9	22173407	<i>CDKN2B-AS1</i>	2	0	0.00	2
High-grade Serous + Endometriosis	rs13000026	chr2	165558884	<i>COBLL1</i>	1	0	0.00	1
LMP Serous + Endometriosis	rs4654785	chr1	22491843	<i>LOC105376850</i>	5	0	0.00	5
LMP Serous + Endometriosis	rs10748858	chr10	105639514	<i>OBFC1</i>	4	0	0.00	4
LMP Serous + Endometriosis	rs11031005	chr11	30226356	<i>FSHB</i>	2	0	0.00	2
Low-grade Serous + Endometriosis	rs77294520	chr2	11660955	<i>GREB1</i>	1	0	0.00	1
Low-grade Serous + Endometriosis	rs584336	chr6	152616173	<i>SYNE1</i>	1	0	0.00	1
Mucinous + Endometriosis	rs6546324	chr2	67856490	<i>LINC01812</i>	3	0	0.00	3
Mucinous + Endometriosis	rs67808862	chr3	138849543	<i>BPESC1</i>	2	0	0.00	2

nOverlap: number of SNPs in locus intersecting biofeature.